

**GEOMORPHOLOGY OF THE NORTHEAST PLANNING AREA,  
NATIONAL PETROLEUM RESERVE—ALASKA, 2003**

THIRD ANNUAL REPORT

Prepared for

**ConocoPhillips Alaska, Inc.**  
P.O. Box 100360  
Anchorage, AK 99510

and

**Anadarko Petroleum Corporation**  
3201 C Street, Suite 603  
Anchorage, AK 99503

Prepared by

M. Torre Jorgenson  
Erik. R. Pullman

**ABR, Inc.—Environmental Research & Services**  
PO Box 80410  
Fairbanks, AK 99708

and

Yuri L. Shur

**Department of Civil Engineering**  
University of Alaska  
PO Box 755900  
Fairbanks, AK 99775

January 2004





## TABLE OF CONTENTS

List of Figures.....	i
List of Tables.....	iii
List of Appendices.....	iii
Acknowledgments.....	iii
Introduction.....	1
Methods.....	2
Floodplain Development On Fish and Judy Creeks.....	2
Sedimentation, Permafrost, and Riverbank Erosion Near the Nigliq Channel Crossing.....	4
Ice Wedge Degradation.....	4
Field Surveys of Microsite Changes.....	4
Photointerpretation of Degradation stages.....	6
Spectral Analysis of Extent of Degradation.....	6
Results and Discussion.....	7
Floodplain Development On Fish and Judy Creeks.....	7
Soil Stratigraphy and Sediment Characteristics.....	7
Ice Structures and Volumes.....	11
Floodplain Accumulation Rates.....	14
Sedimentation, Permafrost, and Riverbank Erosion Near the Nigliq Channel Crossing.....	16
Sedimentation.....	16
Permafrost.....	16
Riverbank Erosion.....	18
Ice-wedge degradation.....	18
Field Surveys of microsite changes.....	18
photointerpretation of degradation stages.....	26
Spectral Analysis of Extent of Degradation.....	28
Factors Affecting Degradation.....	32
Summary and Conclusions.....	32
Floodplain Development On Fish and Judy Creeks.....	32
Sedimentation, Permafrost, and Bank Erosion Near the Negliq Channel Crossing.....	33
Ice Wedge Degradation.....	33
Literature Cited.....	35

## LIST OF FIGURES

Figure 1. Soil sampling locations for the floodplain development and ice wedge degradation studies in the Northeast Planning Area, NPRA, 2003.....	3
Figure 2. Soil sampling locations for sedimentation and permafrost characteristics near the proposed road alignment in the western Colville Delta.....	5
Figure 3. Oblique airphotos of the meander floodplain along Fish Creek in the Northeast Planning Area, NPRA.....	8
Figure 4. Soil stratigraphy along a floodplain toposequence in the eastern portion of the Northeast Planning Area, NPRA, 2003.....	9
Figure 5. Soil stratigraphy along a floodplain toposequence in the central portion of the Northeast Planning Area, NPRA, 2003.....	10
Figure 6. Relative distribution of ice structures by lithofacies and by surface terrain unit for fluvial soils in the Northeast Planning Area, NPRA, 2003.....	12

Figure 7.	Depth profiles of electrical conductivity and pH by surface terrain unit, Northeast Planning Area, NPRA, 2003.....	13
Figure 8.	Mean volumetric ice contents grouped by primary ice structure, lithofacies, and surface terrain unit, Northeast Planning Area, NPRA, 2003 .....	14
Figure 9.	Depth profiles of volumetric ice and dry density by surface terrain unit, Northeast Planning Area, NPRA, 2003 .....	15
Figure 10.	Mean accretion rates of surface materials on inactive and abandoned floodplains along Fish Creek, Northeast Planning Area, NPRA, 2003.....	16
Figure 11.	Photographs of soil profiles taken in 1996 and 2003 illustrating sediment deposits associated with overbank flooding in 1989, 1993, and 2000 along the Negliq Channel in the Colville Delta, 2003.....	17
Figure 12.	Mean depth to and thickness of sediment deposits associated with overbank flooding in 1989, 1993, and 2000 along the Negliq Channel in the Colville Delta, 2003 .....	18
Figure 13.	Soil and ice stratigraphy of three cores obtained along the proposed road alignment across the Nigliq Channel, western Colville Delta, 2003 .....	19
Figure 14.	Potential mean thaw settlement estimates for delta inactive floodplain deposits if the active layer increased to either 80 or 110 cm after severe surface disturbance, Colville Delta, 2003.....	20
Figure 15.	Rates of bank erosion near the proposed road alignment across the Nigliq Channel, western Colville Delta, 2003 .....	20
Figure 16.	Views of ice wedges at bank exposures illustrating the thin layer of organic and mineral material over massive ice, and sediment deformation between ice wedges, Northeast Planning Area, NPRA, 2003.....	21
Figure 17.	Ground views of six stages of ice-wedge degradation. Stages are: undegraded troughs, initial, intermediate, and advanced degradation, initial, and advance stabilization .....	23
Figure 18.	Photographs of soil profiles illustrating changes in soil stratigraphy and ice structures associated with six stages of ice-wedge degradation, Northeast Planning Area, NPRA, 2003. ....	24
Figure 19.	Changes in mean trough depths, water depths, thaw depths, thickness of new sedge peat, thickness of soil above wedge ice, and thickness of various ice structures associated with six stages of ice-wedge degradation, Northeast Planning Area, NPRA .....	25
Figure 20.	Abundance of thermokarst pits on airphotos taken in 1945, 1982, and 2001 within two 250 × 250 m areas, Northeast Planning Area, NPRA, 2003.....	27
Figure 21.	Percent area and density of thermokarst pits associated with ice-wedge degradation evident on airphotos taken in 1945, 1982, and 2001 for two small map areas, Northeast Planning Area, NPRA, 2003.....	28
Figure 22.	Changes in flooded areas in the west change study region 1945 and 2001 used to differentiate areas of thermokarst, Northeast Planning Area, NPRA, 2003. Small waterbodies present only in 2001 are attributed to thermokarst.....	29
Figure 23.	Changes in flooded areas in the central change study region between 1945 and 2001 used to differentiate areas of thermokarst, Northeast Planning Area, NPRA, 2003 .....	30
Figure 24.	Summary of changes in flooded areas between 1945 and 2001 by terrain unit and physiography for the central and western map areas, Northeast Planning Area, NPRA, 2003 .....	31
Figure 25.	Mean annual air temperatures for Barrow Alaska, 1921–2003 .....	34

**LIST OF TABLES**

Table 1. Characteristics of six stages of ice-wedge degradation in Northeast Planning Area, NPRA, Alaska, 2003 ..... 22

**LIST OF APPENDICES**

Appendix 1. Classification and description of lithofacies observed in North Slope soils, 2003..... 38  
Appendix 2. Description of ground ice structures observed in the NPRA study area, 2003 ..... 40

**ACKNOWLEDGMENTS**

This study was funded by ConocoPhillips Alaska, Inc., and managed by Caryn Rea, Environmental Studies Coordinator. We also would like to acknowledge the assistance of J. J. Frost, Luke McDonough, and Gerrit Vyn who helped with the coring. Doreen Nupigiak of research liason for Nuiqsut also observed our work and was very helpful. James Talik of Nuiqsut provided great help with logistics. Janet Kidd technically reviewed the report.



## INTRODUCTION

Permafrost development on the Arctic Coastal Plain in northern Alaska greatly affects the ecological conditions at the ground surface (Billings and Peterson 1980, Webber et al. 1980, Walker 1981), the engineering properties of the soil (Johnson 1981, Kreig and Reger 1982, McFadden and Bennet 1991), and the response of the terrain to human activities (Brown and Grave 1979, Webber and Ives 1978, Lawson 1986). Of particular interest for assessing potential impacts from oil development in the National Petroleum Reserve–Alaska (NPRA) are the identification of terrain relationships for predicting the nature and distribution of ground ice across the landscape, and an evaluation of how permafrost will respond to disturbance. Accordingly, this study was designed to (1) determine the nature and abundance of ground ice at multiple spatial scales to develop terrain relationships for predicting ice distribution, (2) assess flood sedimentation, permafrost characteristics, and riverbank erosion along the proposed road alignment on the floodplain of the western Colville Delta, and (3) assess the rates of landscape change associated with ice-wedge degradation.

While there is consensus that the soils of the Arctic Coastal Plain have high ice contents, little information is available on the nature, distribution, and dynamics of ground ice. Kreig and Reger (1982) provided a comprehensive analysis of relationships between landforms and soil properties, but their data do not allow the prediction of ice distribution across the coastal plain. At Barrow, the volume of segregated ice in the surface soils often approached 80% (Brown 1968) and overall ice content associated with segregated ice averaged 62% (Hinkel et al. 1996), but the relationship between ice content and terrain characteristics were not examined. On the Mackenzie River Delta, pore and segregated ice occupied 80% of the soil matrix and wedge ice constituted 12–16% of total volume of the surface soils (Pollard and French 1980), and the structure of the ice has been well documented (Murton and French 1994). Studies of the nature and distribution of ground ice on the Colville River Delta showed that ice content was strongly related to ice structure, soil texture, and terrain unit

(Jorgenson et al. 1997a, Jorgenson et al. 1998). The mean total volume of segregated ice for the most ice-rich terrain unit, abandoned floodplains, was 79%. Similarly, a study of ground ice patterns and thermokarst potential in the Prudhoe Bay and Kuparuk oilfields found that the mean volume of segregated ice in alluvial plain deposits was 76% (Burgess et al. 1998). Our efforts in 2003 expanded upon the work conducted in 2001–2002, which focused on describing terrain units associated with lake basin development (Jorgenson et al. 2002, 2003a), to include identifying the patterns and processes of permafrost development on the floodplains of Fish and Judy creeks. We examined the process of natural degradation of ice wedges, which typically occupy 10–20% of the volume of surficial materials on the Beaufort Coastal Plain, and assessed ice volumes along the proposed road alignment within the Colville River Delta.

To address design concerns associated with road access to oilfield facilities in the NPRA, we also focused on the sedimentation, permafrost characteristics, and riverbank erosion along a proposed road alignment that would cross the Nigliq Channel. Sediment deposition on the Colville Delta floodplain is critically important for maintaining productive habitats and contributes fine-grained sediments responsible for the development of very ice-rich soils on the delta (Jorgenson et al. 1997a, 1997b). Thus, information on the relationship of sedimentation to recent overbank flooding can be used to assess potential impacts of the proposed road on sediment deposition above and below the proposed road. Information on ground ice volume and potential for thermokarst is important for evaluating the potential consequences of disturbances associated with the road, including dust, impoundments, and off-road travel. This evaluation compliments earlier, more intensive studies on geomorphic processes in the delta (Jorgenson 1996, 1997a).

While naturally occurring thermokarst is fundamental to ecological processes in arctic lowlands (Britton 1957, Billings and Peterson 1980, Walker et al. 1980, Carter et al. 1987), human-induced thermokarst is a concern for land development in the Arctic because of the subsequent changes in hydrology, soils, and vegetation (Brown and Grave 1979, Jorgenson

1986, Lawson 1986, Walker et al. 1987). In the context of oil development activities, of specific concern is the possibility of thermokarst as a result of off-road and seismic trail disturbances (Walker et al. 1987, Emers and Jorgenson 1997); alteration of drainage patterns following road development, road dust, oil spill cleanups (Jorgenson et al. 1991, Jorgenson et al. 1992); closeout and rehabilitation of reserve pits (Burgess et al. 1999); and gravel removal after site abandonment (Jorgenson and Kidd 1991, Kidd et al. 1997). Thus, to develop land rehabilitation strategies that are site-specific and appropriate to the rapidly changing environmental conditions associated with thermokarst, it is essential to understand the nature and abundance of ground ice in areas proposed for development, and to relate ice characteristics to terrain characteristics at a level useful for land management. While previous research in 2001–2002 focused on thaw settlement characteristics of segregated ice associated with various terrain units (Jorgenson et al. 2003a), efforts in 2003 focused on the process of natural degradation of ice wedges, which typically occupy 10–20% of the volume of surficial materials on the Beaufort Coastal Plain.

To provide a framework for sampling and analyzing the spatial variability of ground ice across the landscape, and to identify the geographic scales most useful for interpretation and management, we used a hierarchical approach that incorporated regional, landscape, and local ecosystem scales. At the regional level, we used ecodistricts and ecosubdistricts (associations of terrain units and geomorphic processes) developed by Jorgenson et al. (1997b) as the basis for allocating our sampling effort. At the landscape scale, we used terrain units (depositional units related to a specific geomorphic process) to stratify our sampling and as the basis for analysis. At the local ecosystem level (areas with relatively uniform soil stratigraphy and vegetation), we classified our samples (soil cores) using micro-scale characteristics such as ice structure and lithofacies (texture and structure) for analysis.

Specific objectives of this study were to:

1. determine differences in soils and ground ice among terrain units to evaluate sedimentation and permafrost changes during floodplain development

along Fish Creek,

2. quantify sedimentation, permafrost, and riverbank erosion characteristics near the Nigliq channel crossing to assist the engineering design of the proposed road alignment and to assessing its potential environmental consequences; and
3. evaluate the process of natural ice-wedge degradation to better assess the potential for thermokarst after disturbance.

## METHODS

### FLOODPLAIN DEVELOPMENT ON FISH AND JUDY CREEKS

Field surveys were conducted during 31 July–8 August 2003 to characterize the soil and ice stratigraphy along three transects (toposequences) and at two bank exposure sites on the Judy and Fish Creek floodplains (Figure 1). The sites were subjectively chosen to include a variety of floodplain terrain types. These toposequences are a surrogate for evaluating changes over time and thus provide a record of terrain development on the meandering floodplains.

At each toposequence, 5–7 soil cores were collected, (depending on the number of terrain types), for a total of 16 cores. The stratigraphy of the near-surface soil (i.e., the active layer) was described from soil pits to assess the depth of thaw, surface organic thickness, and mineral characteristics. Below the active layer, profiles were described from 2–2.7 m long frozen cores obtained using a 7.5-cm-diameter SIPRE corer with a portable power head. At the two bank exposures, profiles were described after unfrozen material was removed with a shovel to expose undisturbed frozen sediments. Descriptions for each profile included the texture of each horizon, the depth of organic matter, depth of thaw, and visible ice volume and structure. In the field, soil texture was classified according to the Soil Conservation Service system (SSDS 1993).

Soil samples were taken every 20–30 cm from 16 core sections and the two exposures, within soil horizon boundaries (total of 194 samples). Samples were analyzed for volumetric and gravimetric water content, electrical conductivity,

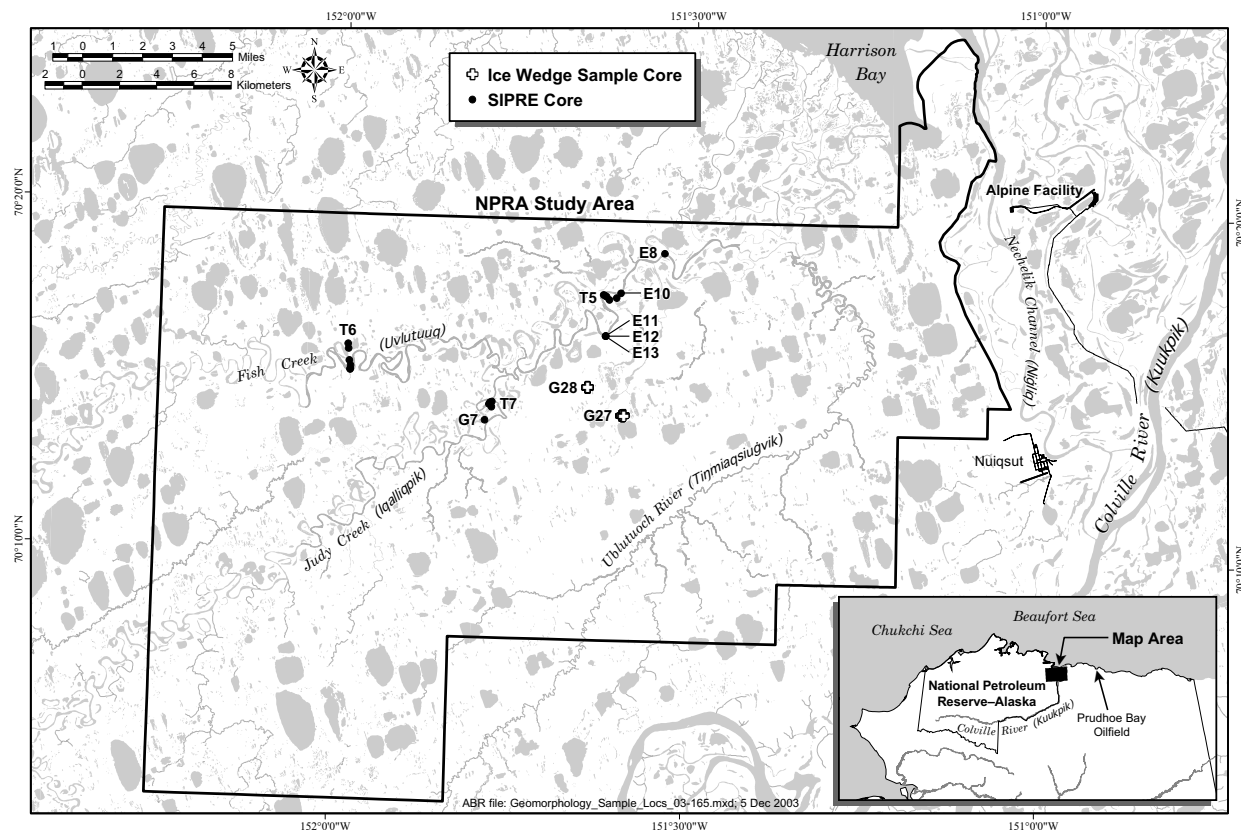


Figure 1. Soil sampling locations for the floodplain development and ice wedge degradation studies in the Northeast Planning Area, NPR, 2003.

and pH. The soil volume of each SIPRE core sample was determined by multiplying the average length of three sides of the sample by the area of the core (derived from its circumference). A metal sample ring was used to obtain volumetric samples at exposures. EC was measured using an Orion model 290 EC meter and pH was determined using an Orion model 290 pH meter. Total carbon (results pending) was determined on a subset of soil samples by the Palmer Research Station Soils Laboratory (Palmer, AK).

To establish minimum ages for the older stratigraphic terrain units, one sample of basal organic material was collected from two cores in 2003. Laboratory analysis was performed by Beta Analytic, Inc. (Coral Gables, FL). Dates in this report are presented as calibrated calendar ages, years before present (BP, base 1950) and include the range associated with the 2 sigma error (Stuiver et al. 1998).

The micro-scale soil textures and structures described from the field profiles were grouped into

lithofacies (distinctive suites of sedimentary structures related to a particular depositional environment), and cryostrucures (repeating patterns of ice distribution). These field descriptions were subsequently reviewed for consistency in the office using field descriptions and photographs of cores. Lithofacies were classified according to systems of facies analysis for fluvial deposits developed by Miall (1978, 1985) and Brierley (1991) and modified to incorporate features specific to the permafrost environment (Jorgenson et al. 2002)(Appendix Table 1). Ice structure (primary continuity, secondary shape or orientation, and tertiary size) was classified in the field in 2003 following a version of the system developed by Murton and French (1994), but modified to better differentiate the structures that we observed on the Colville Delta (Jorgenson et al. 1997a)(Appendix Table 2). Terrain units were classification according to the systems developed by Kreig and Reger (1982) and the Alaska Division of Geological and Geophysical

Surveys, but modified to incorporate the surficial geology units mapped for the area by Carter and Galloway (1985). A more complete discussion of classification is presented in Jorgenson et al. 2003.

### **SEDIMENTATION, PERMAFROST, AND RIVERBANK EROSION NEAR THE NIGLIQ CHANNEL CROSSING**

Sediment deposition associated with three large flood events (1989, 1993, and 2000) was measured at 25 locations above and below the proposed road alignment crossing the Nigliq Channel in the western Colville Delta during mid-August 2003 (Figure 2). Most of the sampling was done at locations previously surveyed in 1996 (Jorgenson et al. 1997a) so sedimentation layers could be compared between 1996 and 2003 at most locations. At each location, a soil plug was extracted from the active layer and measurements were made of the depth to the top of each distinct sediment layer and the thickness of each layer. The distinctness of each boundary and the texture of the sediment were noted. A photograph was taken of each soil plug. In the office, field measurements and photographs were reviewed and each sediment layer near the surface was assigned a year associated with one of three major overbank floods during the last 15 years. Soil surveys in 1992 (Jorgenson et al. 1993) also were used for reference when assigning flood events.

Permafrost properties were described at three locations on the floodplain of the Colville Delta along the proposed road alignment just west of the Nigliq Channel on 7 August 2002 (Figure 2). The stratigraphy of the near-surface soil (i.e., the active layer) was described from soil pits and included recording the depth of thaw, surface organic thickness, and mineral characteristics. For sampling frozen soils below the active layer, the SIPRE corer described above was used to obtain ~2.5 m cores. Descriptions for each profile included the texture of each horizon, the depth of organic matter, depth of thaw, and visible ice volume and structure. In the field, soil texture was classified according to the Soil Conservation Service system (SSDS 1993). Soil samples were taken from each stratigraphic section from the three cores sections (total of 49 samples). Samples were analyzed for volumetric and gravimetric

water content, electrical conductivity, and pH. The volume of the frozen sample was determined as described above for the sediment cores. EC was measured using an Orion model 290 EC meter and pH was determined using an Orion model 290 pH meter.

Rates of riverbank erosion along the Nigliq Channel near the proposed road alignment west to the NPRA were determined by comparing shorelines evident on 1955 and 2001 photography. The 1955 black and white photography (24 July 1955, 1:50,000 scale) was scanned and orthorectified to the 2001 true-color orthophoto mosaic produced by Aeromap, Inc. (nominal scale 1:18,000). The riverbanks then were digitized from both sets of photography. After digitizing, the length between the two shores lines was measured at 10 locations 100-m apart.

### **ICE WEDGE DEGRADATION**

The evaluation of ice-wedge stability and degradation was conducted at three scales: (1) field surveys were conducted in August 2002 and 2003 to assess changes in vegetation and soil properties associated with ice-wedge degradation at the microsite scale; (2) degradation stages were delineated and classified within two small (6.25 ha) mapping areas over a time series of photographs taken in 1945, 1982, and 2001 at the site scale; and (3) waterbodies associated with thermokarst were classified by spectral analysis within two larger (1450 ha) mapping areas to assess the extent of degradation and its dependence on terrain units at the landscape scale. The the small area mapping was done in 2003, and the spectral analysis of larger areas was done in 2002.

### **FIELD SURVEYS OF MICROSITE CHANGES**

Field surveys were conducted at 10 locations within two general areas in 2002 (C5 and C6) and at 33 locations within two general areas (G27 and G28) in 2003 (Figure 2). At all locations, a soil plug of the active layer was removed by hand and a core of the frozen soil and top of the wedge ice was obtained with a 7.5-cm-diameter SIPRE core. Photographs of the ground view and soil profile were taken at each site. Thaw depth, water depth, trough depth (difference between height of polygon centers to bottom of trough), and depth to wedge ice were recorded at each site, if applicable.

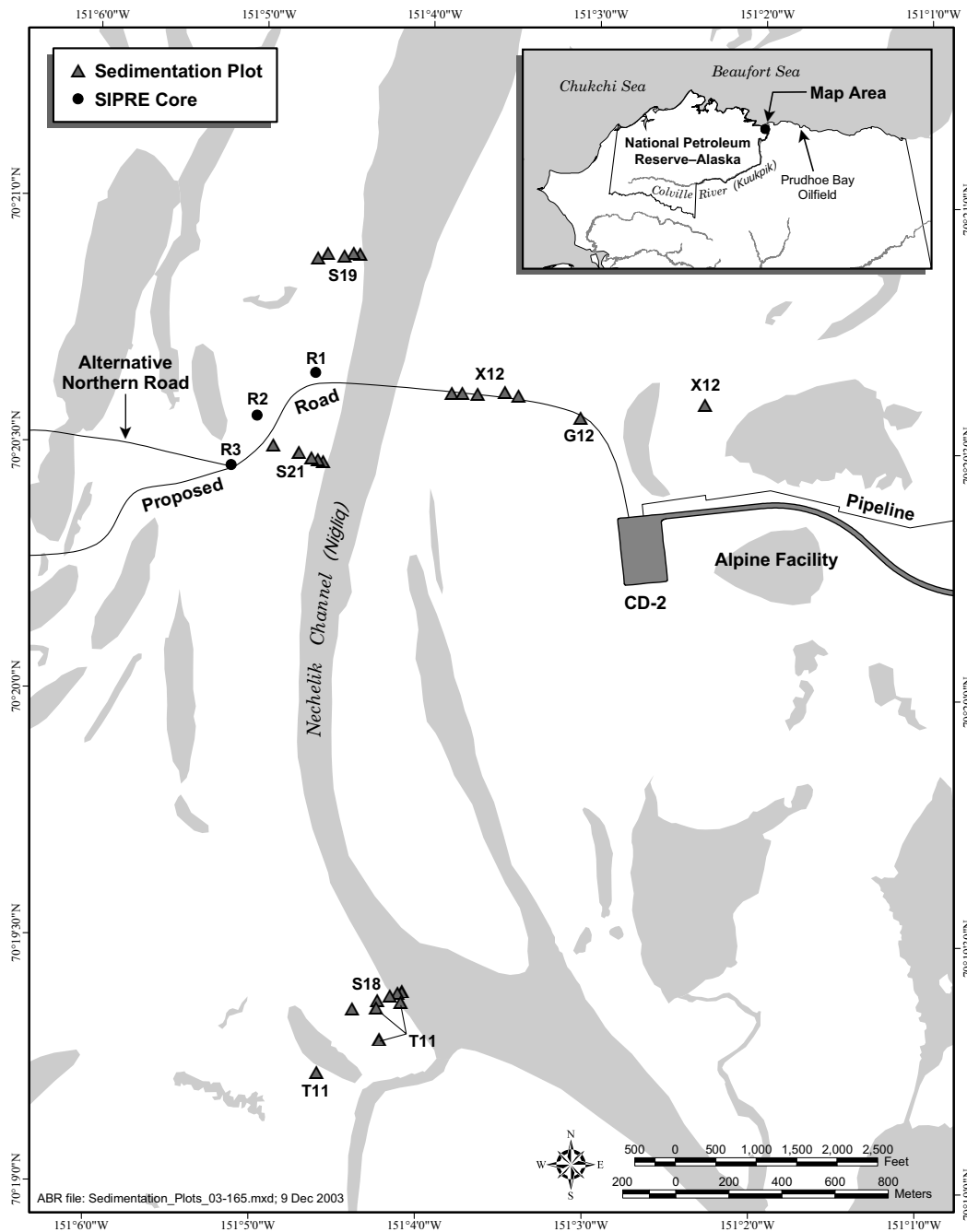


Figure 2. Soil sampling locations for sedimentation and permafrost characteristics near the proposed road alignment in the western Colville Delta, 2003.

In 2003, the thickness of sedge peat accumulating above dead tussocks and a listing of dominant plant species at the survey sites also was recorded. For the sites surveyed in 2002, sedge peat thickness was measured by reviewing the soil photos and using the measuring tape in the photo for scale.

During the survey, each site was classified into one of six degradation stages based on

vegetation, water depth, and trough depth. These stages include: (1) *undegraded* troughs with no evident change in tussock tundra condition; (2) *initial degradation* with slight greening of tussocks but little settlement; (3) *intermediate degradation* with robust green tussocks; some settlement, and shallow standing water; (4) *advanced degradation* with no vegetation, deep water, and large amount

settlement; (5) *initial stabilization* with the presence of robust aquatic sedges in shallow water, and (6) *advanced stabilization* with development of less robust sedges and mosses with little or no standing water.

#### PHOTOINTERPRETATION OF DEGRADATION STAGES

Linear depressions with standing water or wet sedge vegetation associated with ice-wedge degradation were mapped for two small areas (250 × 250 m) on aerial photography from 4 July 1945 (NARL series, 1:45,000 scale black and white), July 1982 (Alaska High Altitude Program, 1:63,000 scale), and 13 July 2001 (Aeromap, Inc., nominally 1:18,000 true-color used to create a digital orthophoto mosaic). Aerial photographs from 1945 and 1982 were scanned and georectified to the July 2001 orthophoto mosaic using stable features (polygonized tundra intersections, stable lake peninsulas) common to both the old and recent photography. Minimum mapping size was 4 m<sup>2</sup> for 1945, 12 m<sup>2</sup> for 1982, and 2 m<sup>2</sup> for 2001.

During mapping of the thermokarst pits on the three sets of photographs for the two sites, each polygon was coded with area, year, and degradation stage (initial and intermediate stages were omitted because they were not consistently evident). For analysis, the number and aerial extent of polygons were computed for each year and area. The scale (and resolution) of the photography varied among the years analyzed, so we established a minimum polygon size of 12 m<sup>2</sup> (size mappable in 1982) to make the comparison of waterbodies consistent across the various scales. However, calculations were made for all polygons visible in the 2002 photography.

#### SPECTRAL ANALYSIS OF EXTENT OF DEGRADATION

In 2002, spectral analysis of ice-wedge degradation was performed for two of the three small study areas (central and west, 1450 ha each) to compare waterbody changes between 1945 and 2001 (Jorgenson et al. 2003a). Spectral analysis was not conducted with the 1982 photography because the scale was too small to consistently differentiate thermokarst pits and because the spectral classification for shallow waterbodies was poor. The ecological land survey (ELS) map was

used to exclude non-terrestrial areas (lakes and streams) from the analysis because wave reflection (in 2001 photography) and late season ice (in 1945 photography) interfered with spectral classification of larger waterbodies.

Inundated tundra areas were determined using image-processing techniques to identify areas of “deep” (>30 cm) water that were typical of the thermokarst pits observed in the field. All image analysis was performed with Imagine 8.2 (ERDAS, Inc.). For the 1945 photography, the controlled digital image was balanced to account for systematic illumination variation across the photo. Water was differentiated by choosing the grayscale value that most commonly depicted the transition from wedge sedge meadow tundra (water < 10 cm deep) to deeper water areas. All grayscale values in the digital image below this number were coded to 1, while all remaining areas were coded to 0. Threshold values for each image were chosen by examining the extent of water in all terrain types, but preference was given for a threshold value that most accurately delineated small waterbodies on Alluvial-marine Terrace and Eolian inactive sand deposits. In establishing a threshold, we intended to be conservative to bias toward differentiating deeper water to avoid including very shallow water on wet tundra.

Because the 2001 digital image consisted of three separate bands (true-color image), waterbodies in terrestrial areas were identified using a two-step classification procedure. First, an unsupervised classification was done on the study area sections and each pixel was assigned up to five ranked classes. Second, a fuzzy classification was run to determine the pixel’s most likely class based on surrounding pixel values. The resulting set of classes then was evaluated manually to determine which classes represented deep water areas. For both years, water coverage was calculated for each terrain/surface form combination by summing the pixel areas within each ELS region.

The classified images from both years were used to create a four-class image of each landscape change study region. Each pixel was classified as one of four types: (1) unflooded (not flooded in 1945 or 2001), (2) flooded in 1945, unflooded in 2001, (3) flooded in both 1945 and 2001 or (4) unflooded in 1945, flooded in 2001. Inundated

areas were grouped with upland (well-drained) or lowland (poorly drained) areas by combining surface form designations within terrain types. For example, within Alluvial-marine deposits, upland areas were defined as areas with high-centered, high-relief polygons (Phh) and areas of mixed thaw pits and polygons (Tm). These surface forms represent ice-rich areas where lacustrine processes or other disturbances have been absent for extended periods of time. The ice-rich nature of sediments and predominance of ice wedges make these areas the most sensitive to thermokarst. Areas of high-centered, low-relief polygons (Phl) also are common in swales in upland areas, but frequently are interspersed with low-centered polygons and wetter micro-sites. Thus, this surface form was grouped with lowland types.

## **RESULTS AND DISCUSSION**

### **FLOODPLAIN DEVELOPMENT ON FISH AND JUDY CREEKS**

The classification and mapping of terrain units in 2002 (Jorgenson et al. 2003a, 2003b) differentiated five terrain units associated with the development of meander floodplains along Fish Creek (Uvlutuuq) and Judy Creek (Iqallipik). Of these, four terrain units (meander active fine channel deposits, active overbank deposits, inactive overbank deposits, and abandoned overbank deposits) were directly associated with fluvial processes, while the fifth (eolian inactive sand deposits) was associated with eolian processes in close proximity to barren channel deposits (Figure 3). Based on the results of the toposequences described in 2003, the following section describes those factors that have contributed to changes in terrain characteristics across the floodplain, including comparisons of sediment characteristics, ice structures and volumes, and overall accretion rates of ice and sediment in floodplain soils.

### **SOIL STRATIGRAPHY AND SEDIMENT CHARACTERISTICS**

Changes in elevation, soils, surface-forms, and vegetation were surveyed across two toposequences along Fish Creek and one toposequence along Judy Creek. Transect 5 extends from a riverbar (meander fine active

channel deposit) on Fish Creek inland across eolian inactive sand dunes to inactive overbank deposit terrain (Figure 4). Transect 6 encompasses a complete sequence and extends from a riverbar on Fish Creek over inactive sand deposits to abandoned overbank deposits and to older, higher elevation eolian inactive sand deposits (Figure 5). Transect 7, located on Judy Creek, crossed a toposequence similar to that in Transect 5. These toposequences are a surrogate for evaluating changes over time and thus provide a record of terrain development on the meandering floodplains.

Meander Fine active channel deposits were dominated by retransported inclined or rippled sands that form repeating sequences of medium to fine sand grading upward to very fine sand, indicating frequent scouring and deposition. Soils commonly included a small portion of allochthonous organic material composed of drifted peat that becomes stranded on the surface during waning floods (Figure 5).

Active overbank deposits accumulated in a narrow zone in close proximity to the channel deposits and typically had laminar, interbedded silts and very fine sands, indicating frequent flooding and vertical accretion of sediments. The surface often had small sandy mounds of eolian sand. While the deposits have both fluvial and eolian materials, the deposits are subject to frequent flooding and modification by fluvial processes.

Inactive overbank deposits typically had interbedded organic and very fine sand and silt horizons, indicative of infrequent flooding and sedimentation. Some fine sand may also have been of eolian origin, indicating the deposits are a complex combination of organic matter accumulation and fluvial and eolian deposition. Soil ice structures were a combination of organic, layered, and vein, with ataxitic ice just below the active layer and pore and lenticular ice structures more common at greater soil depths.

Abandoned floodplain cover deposits had thick accumulations of peat at the surface underlain by interbedded sands and organics. Soil horizons often were wavy or disrupted, presumably due to cryogenic soil processes in the active layer and deformation by ice wedge development. Soil ice structures were complex and more developed than



Figure 3. Oblique airphotos of the meander floodplain along Fish Creek in the Northeast Planning Area, NPRA, 2003. Upper photo illustrates complete floodplain development at Transect 6 and lower photo illustrates early floodplain development with large dunes that form behind point bars.

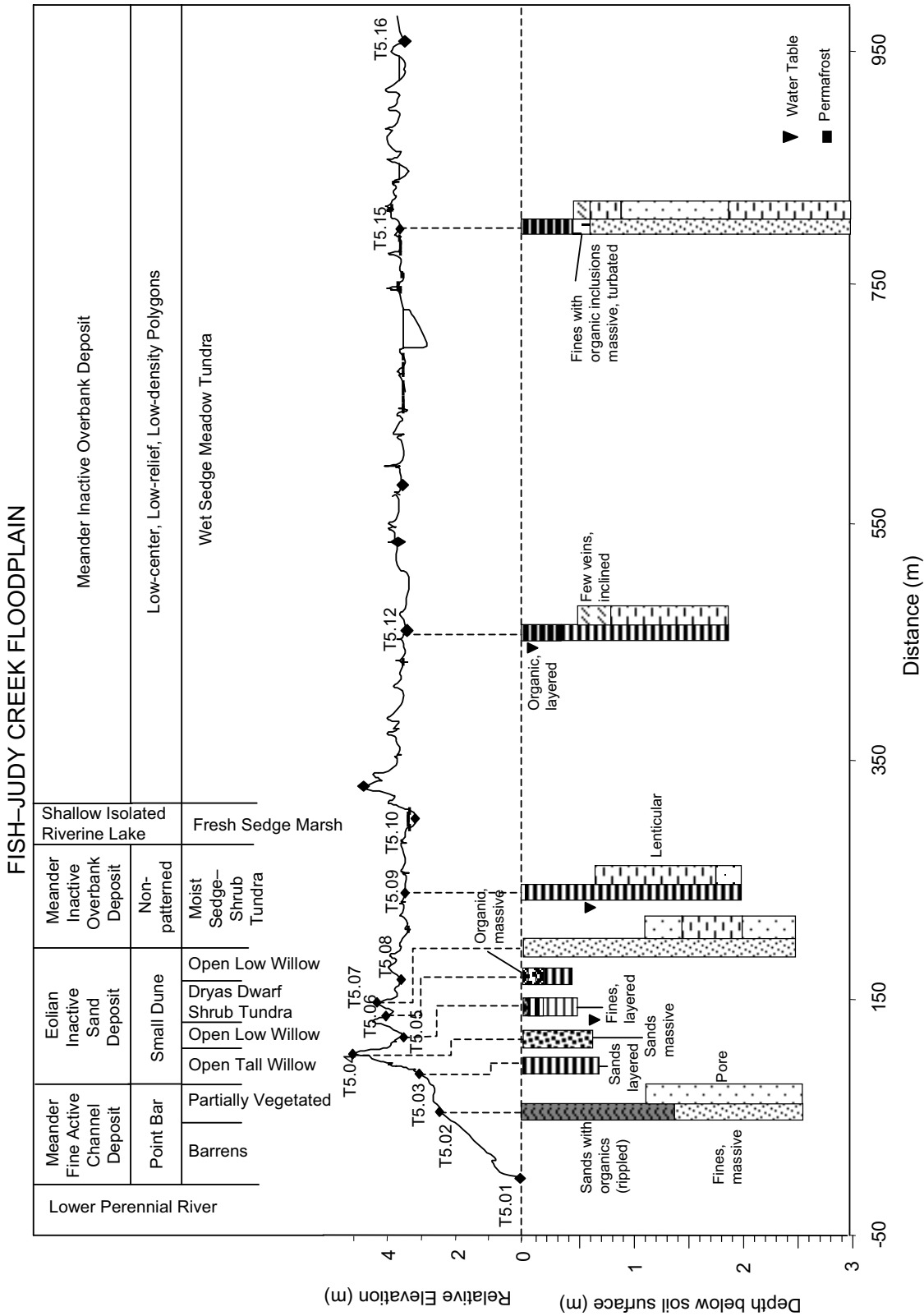


Figure 4. Soil stratigraphy along a floodplain toposequence (Transect 5) in the eastern portion of the Northeast Planning Area, NPRA, 2003.

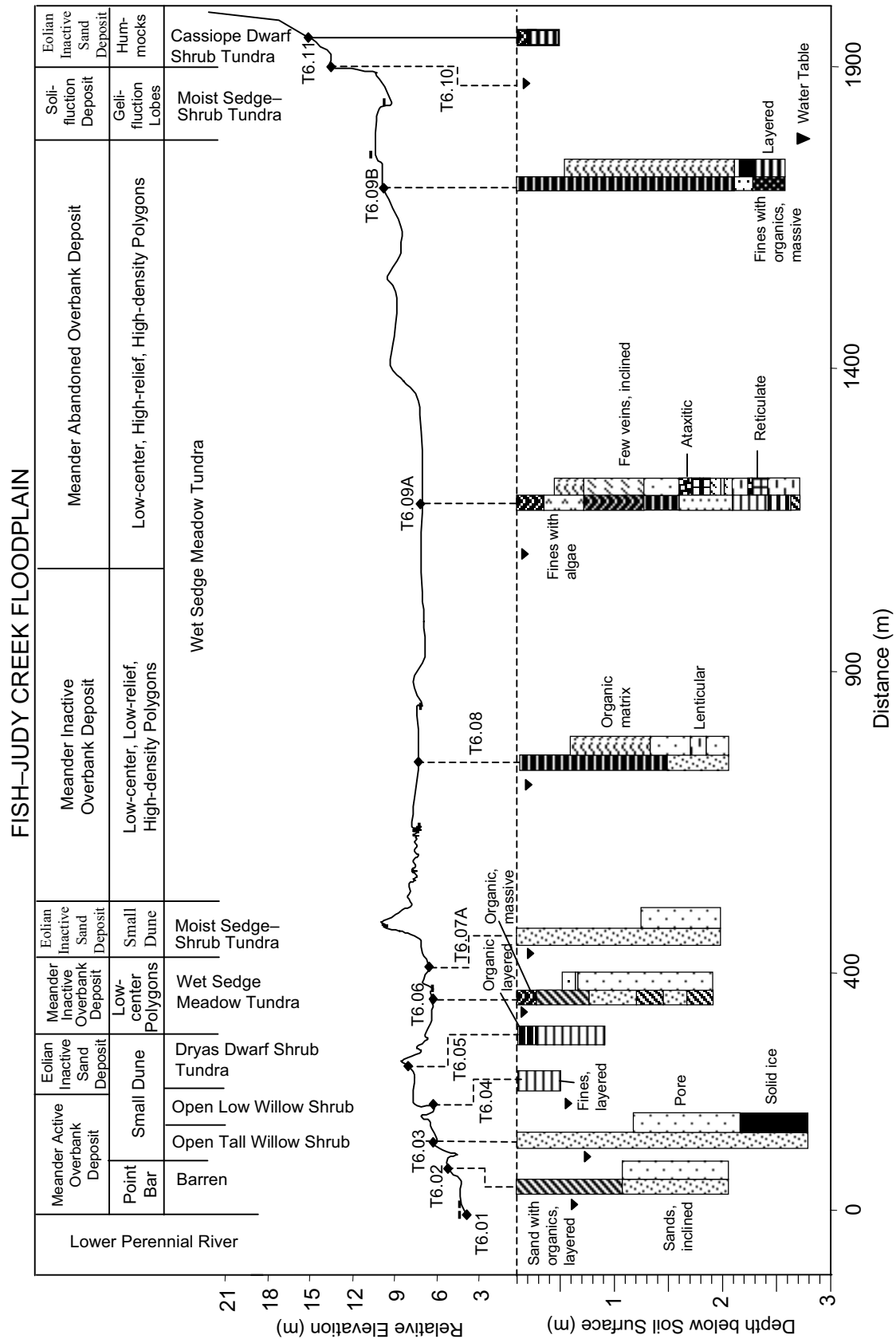


Figure 5. Soil stratigraphy along a floodplain toposequence (Transect 6) in the central portion of the Northeast Planning Area, NPRA, 2003.

in other terrain types in the floodplain due to extensive ground ice formation and advanced ice wedge development. Although these deposits may be flooded occasionally, the deposits at the surface no longer reflect fluvial origin.

Eolian active and inactive deposits usually occurred as distinct streaked dunes comprised of massive and inclined sands. They typically were found in close association with active channel deposits that provided the source areas for the wind blown sand. Active eolian deposits lacked organic matter accumulation at the surface, indicating frequent sand deposition, whereas, inactive deposits had thin organic material horizons or a distinct A soil horizon indicating greater age and lack of active eolian input. Ice structures in the frozen subsurface were dominated by visible and non-visible pore ice and some lenticular ice (Figure 6).

The texture of mineral soils in the Fish and Judy Creek floodplains was dominated by sands eroded from an adjacent Pleistocene sand sheet, and the sediments have been sorted by riverine and eolian processes. Active channel deposits contained the largest particles (typically bedded medium to fine sands). Sediments in eolian inactive sands and active overbank deposits were composed almost entirely of fine to very fine sands. Fines (silts) only appeared in inactive and abandoned overbank deposits and were associated with slackwater flood events or lacustrine processes. Organic material was a minor component of soils in active channel and inactive eolian sand deposits but had a greater presence in active and inactive overbank deposits. Organic material was the dominant soil material in the top meter of abandoned overbank deposits (Figure 5).

Soil pH varied widely across terrain types within the floodplain, with values ranging from 4.7–8.3 (Figure 7). Active channel deposits had pH values ranging from 7.4–8.3, with values increasing with soil depth to a maximum at 1.5 m below the soil surface. In active overbank deposits, pH ranged from 7.4 to 8.2 and tended to decrease with depth. Inactive overbank deposits had highly variable pH values ranging from 6.2–8.3; values tended toward circumneutral with depth. In abandoned overbank deposits, pH values ranged from 4.7–6.9 with values increasing with depth. These trends indicate that carbonates

associated with sediment deposition during early floodplain development cause soils to be alkaline, but as deposits become thicker, receive less flooding and sedimentation, and leach over time, the soils become circumneutral to strongly acidic. Inactive eolian sand deposits had pH values ranging from 7.1 to 8.0 and values varied little with depth (Figure 7).

Salinity, as measured by electrical conductivity (EC) of soil samples obtained from the active layer, were consistently low across the floodplain (Figure 7). EC ranged from 20–130  $\mu\text{S}/\text{cm}$  in active channel deposits and generally decreased with depth (Figure 8). In active overbank deposits, EC ranged from 10–220  $\mu\text{S}/\text{cm}$  and were highest at 1.5 m below the soil surface. Soil EC was highly variable in inactive overbank deposits and ranged from 40–910  $\mu\text{S}/\text{cm}$ ; highest EC values occurred in the active layer (Figure 8). Abandoned overbank deposits had EC values that ranged from 100–570  $\mu\text{S}/\text{cm}$  and generally increased with depth. Soil EC in eolian inactive sand deposits ranged from 60–270  $\mu\text{S}/\text{cm}$  and varied little with depth.

#### ICE STRUCTURES AND VOLUMES

Soil and ice stratigraphy along the terrain sequences from riverbed/sandbar deposits to abandoned overbank cover deposits reflected consistent differences among terrain units (Figure 8). Eight types of cryostructures were observed in sediments: pore, lenticular (tiny ice lenses within the soil matrix), layered (horizontal bedded layers of thin ice), vein (vertically oriented continuous thin veins), reticulate (forming a network), ataxitic (ice with suspended soil inclusions), non-wedge solid ice, and organic (irregular ice within an organic matrix) (Appendix Table 2).

Meander fine active channel deposits contained only visible and non-visible pore structures (ice within the pores of the soil matrix) with ice volumes rarely exceeding the soil pore space. Soil ice development in this terrain is limited due to the young age of the deposit and the coarse size of the sediment (medium to fine sands). Mean ice volume was 37% and ranged from 30.7–47.3% (Figure 8). Soil ice content showed little change with depth in the top 2.5 meters (Figure 9).

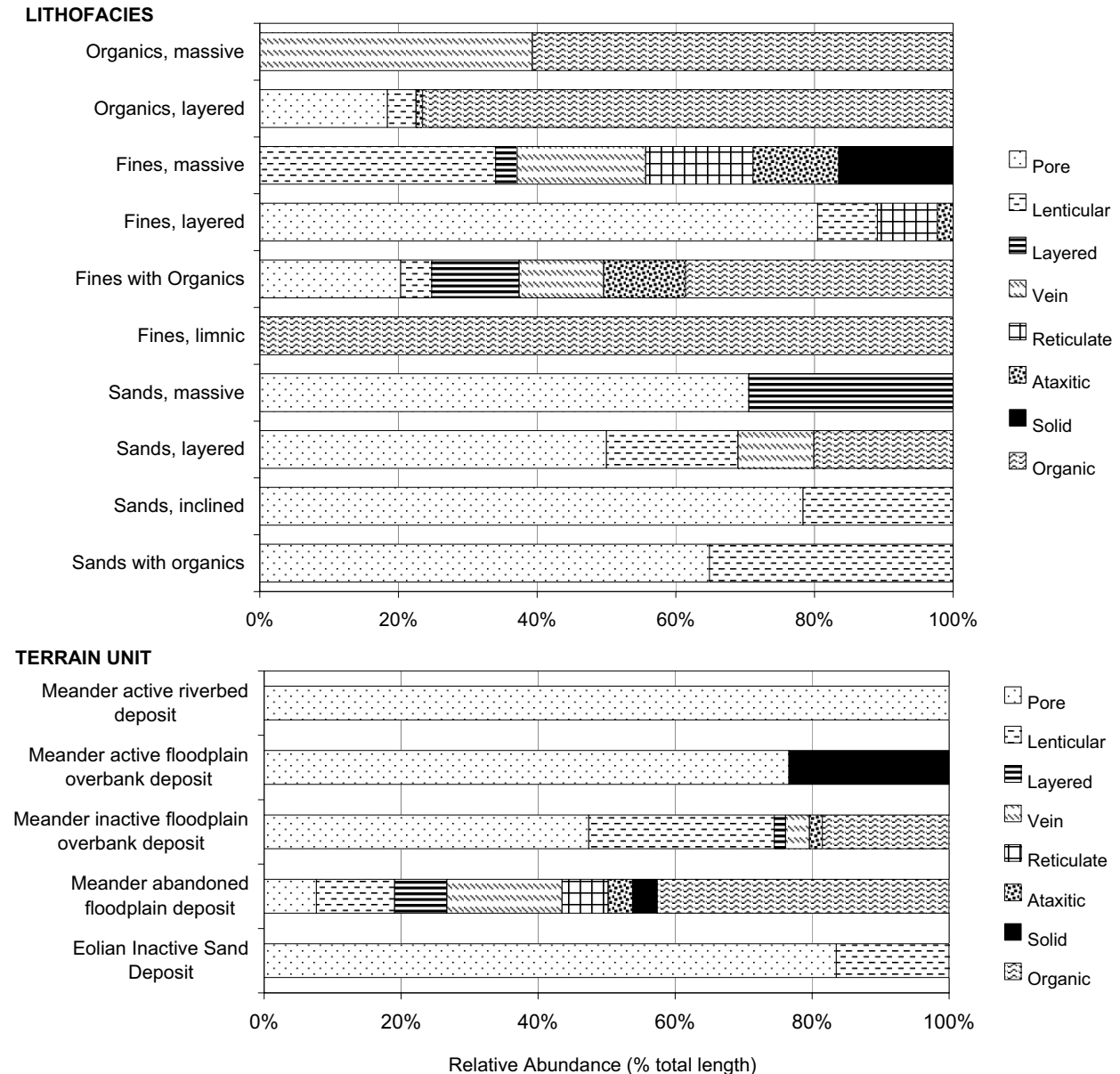


Figure 6. Relative distribution (% of total core length) of ice structures by lithofacies (top) and by surface terrain unit (bottom) for fluvial soils in the Northeast Planning Area, NPRA, 2003..

Meander active floodplain overbank deposits contained mostly visible and non-visible pore ice, although one core (T6.03) collected from this terrain unit included an occurrence of solid ice of uncertain origin (Figure 6). Pore ice in this terrain unit was generally more developed and visible compared to the active channel deposits. Mean ice volume was 37% and ranged from 12–59%, with the exception of 100% in the one core with solid ice (Figure 8). Soil ice content generally increased with depth to 2.5 m (Figure 9).

Inactive overbank cover deposits begin to show more advanced ice aggradation as a result of the accumulation of organic material and slackwater deposition of silts and very fine sands. Soil profiles were still dominated by pore ice, but lenticular, layered, vein, ataxitic, and organic-matrix ice structures also occurred (Figure 6). Mean volumetric ice content was 55% and ranged from 38.1 to 72.7% (Figure 8). Ice content was highly variable and showed no trend with depth (Figure 9). Polygonal rims indicating

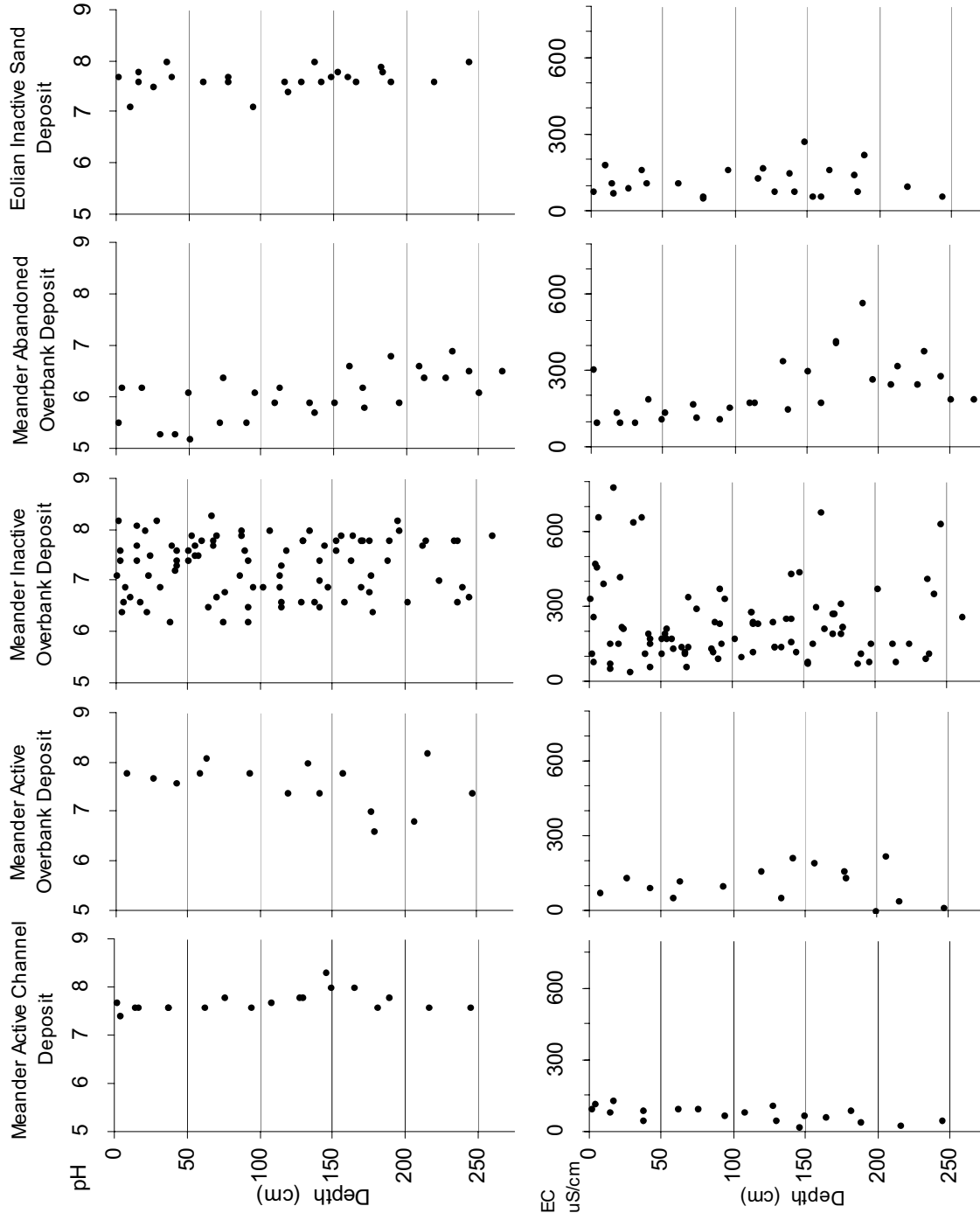


Figure 7. Depth profiles of electrical conductivity (EC) and pH by surface terrain unit, Northeast Planning Area, NPRA, 2003.

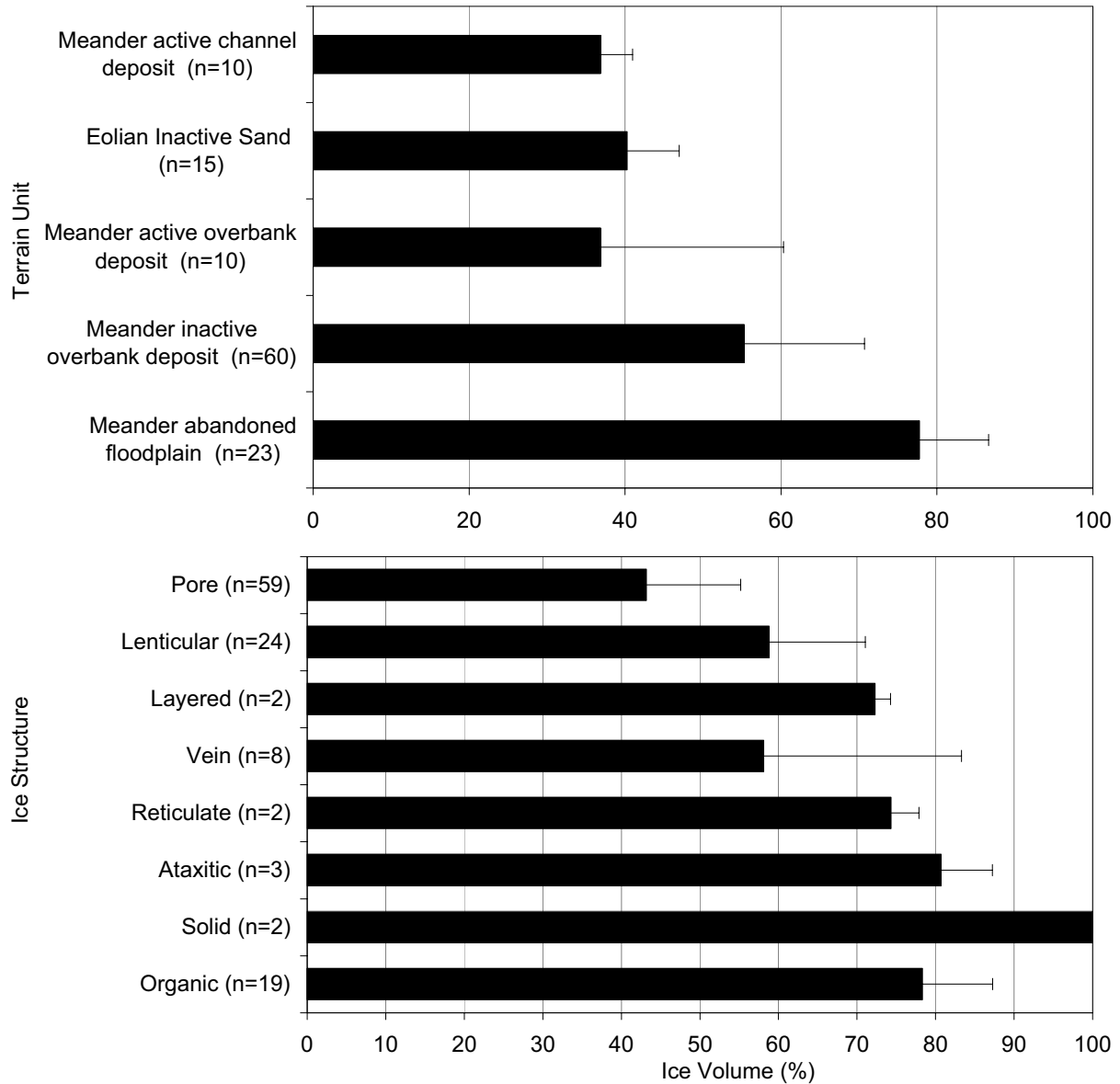


Figure 8. Mean ( $\pm$  SD) volumetric ice contents grouped by primary ice structure (top), lithofacies (middle), and surface terrain unit (bottom), Northeast Planning Area, NPRA, 2003.

ice-wedges were common, although they were low in density.

Abandoned overbank cover deposits generally had complex and well-developed subsurface cryostructures. Ice structure was dominated by organic-matrix ice, but all eight primary structures were observed in soils in this terrain type (Figure 6). Mean volumetric ice content was 78% and ranged from 64.1 to 100% (Figure 8). Ice volumes were generally highest just below the active layer in organic and silt-dominated sediments (Figure 9).

Eolian inactive sand deposits were dominated by pore ice with some areas of lenticular ice in sediments that contained traces of buried organic material. Mean ice volume was 40% and ranged from 29.6 to 43.8% (Figure 8). Ice volumes generally increased with depth (Figure 9).

#### FLOODPLAIN ACCUMULATION RATES

The rate at which material (ice, mineral sediments, and organic matter) has accumulated over time was determined from the two radiocarbon dates obtained from samples retrieved

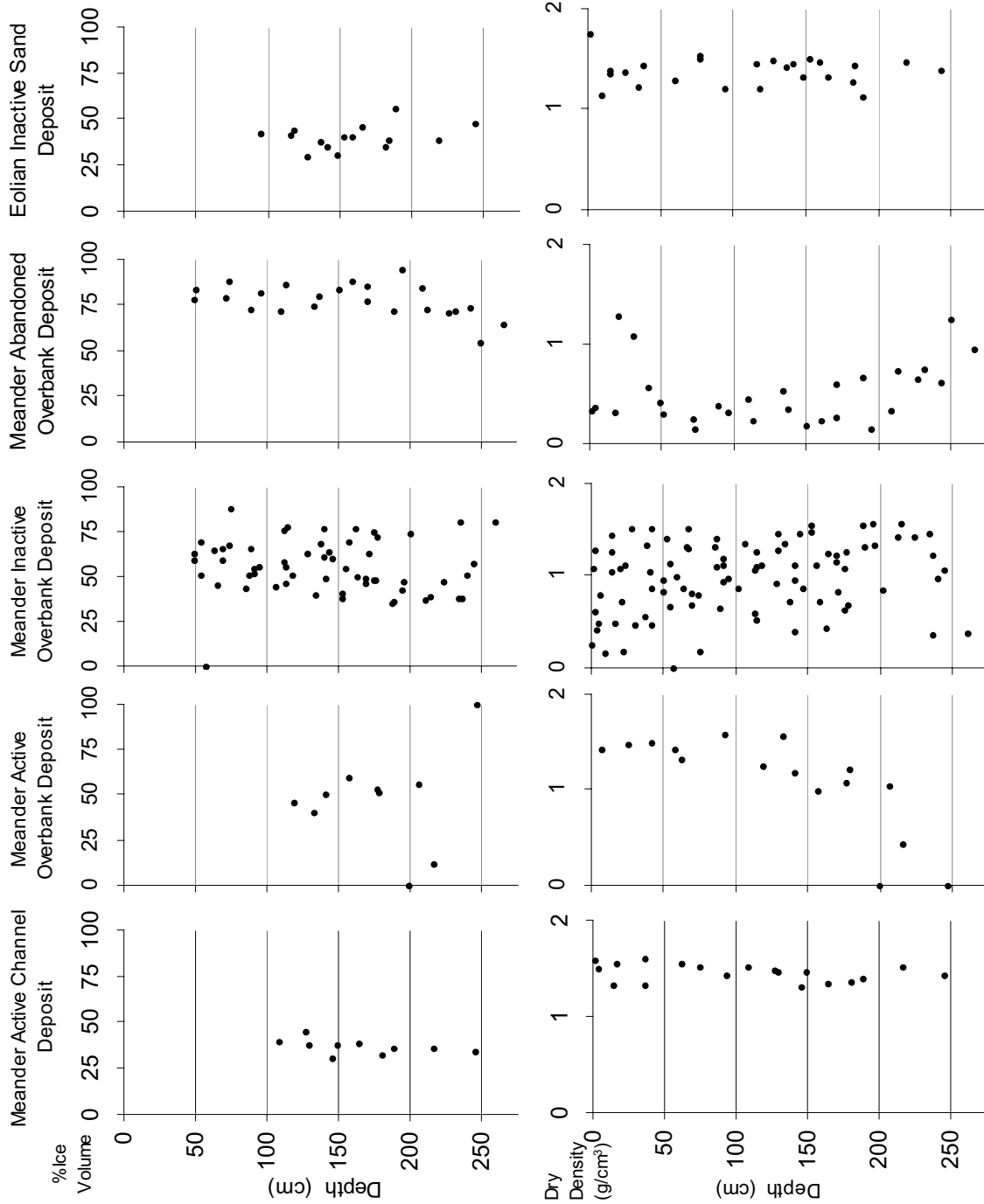


Figure 9. Depth profiles of volumetric ice and dry density by surface terrain unit, Northeast Planning Area, NPRA, 2003.

from core sections and bank exposures. One inactive overbank deposit (E10) had a mean accumulation rate of 0.5 mm/yr, about double that on an abandoned overbank deposit (T6.09b), which had a mean accumulation rate of 0.26 mm/yr (Figure 10).

Accumulation rates were lower than those than the mean rates observed for similar floodplain deposits in the Colville Delta (Jorgenson et al. 1995) (Figure 10). However, the accumulations rates in the Fish and Judy Creek floodplains were greater than many rates observed in other terrain types.

**SEDIMENTATION, PERMAFROST, AND RIVERBANK EROSION NEAR THE NIGLIQ CHANNEL CROSSING**

**SEDIMENTATION**

Sediment layers deposited during overbank flooding in 1989, 1993, and 2000 were evident in most soil cores (Figure 11). Mean thickness of the deposits were 30, 9, and 4 mm, and occurred at mean depth of 6.6, 2.5, and 0.6 cm, respectively (Figure 12). Peak breakup discharges were 379,000 cfs in 1993, 775,000 cfs in 1989 (estimated), and 580,000 cfs in 2000 (Michael

Baker, Jr., 2003). The 1989 estimate was based on elevations of the highest driftlines and hydrologic modeling (Jorgenson et al. 1997a, Shannon and Wilson 1997). The estimated return intervals for these three floods are ~5, ~20, and 100 years, respectively. Thus, the data suggest that 5–10 mm of sediment is deposited every 5–20 years, while rare large events contribute much larger deposits of around 30 mm.

The depositional patterns of infrequent thin deposits and rare thick deposits both have ecological importance for sustaining the relatively high productivity on floodplain environments. The thin deposits contribute periodic nutrient inputs bound to the sediments but are insufficient to damage vegetation. In contrast, the large flood events can smother vegetation, particularly close to the riverbank. While most of the herbaceous vegetation can resprout through the sediment, mosses and lichens are killed by the sediment. Shrubs in particular incur little damage from heavy sedimentation, but rely on the higher levels of nutrient input.

**PERMAFROST**

Soil and ice stratigraphy from three cores from the inactive floodplain adjacent to the

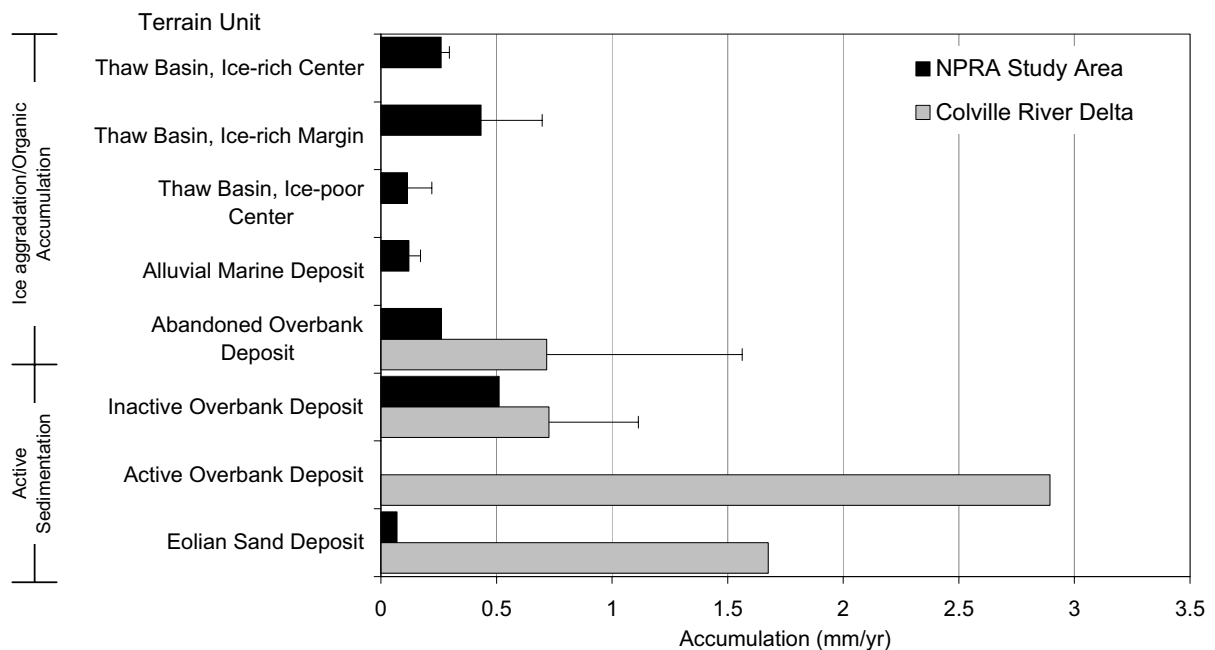


Figure 10. Mean accretion rates (mm/yr) of surface materials (organic, mineral, ice) on inactive and abandoned floodplains along Fish Creek, Northeast Planning Area, NPRA, 2003. Accretion rates were calculated by dividing depth by calibrated radiocarbon age.

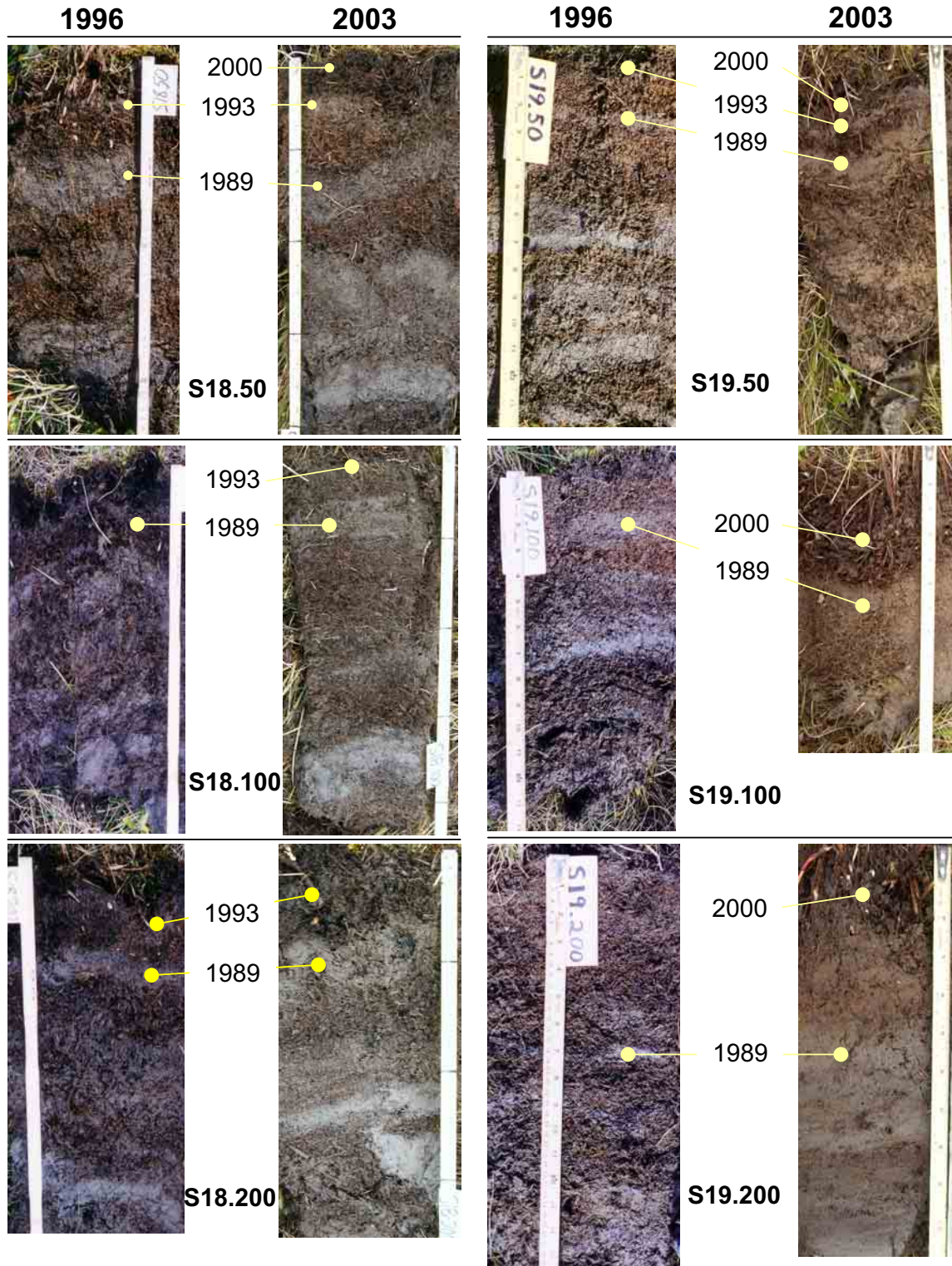


Figure 11. Photographs of soil profiles taken in 1996 and 2003 illustrating sediment deposits associated with overbank flooding in 1989, 1993, and 2000 along the Negliq Channel in the Colville Delta, 2003.

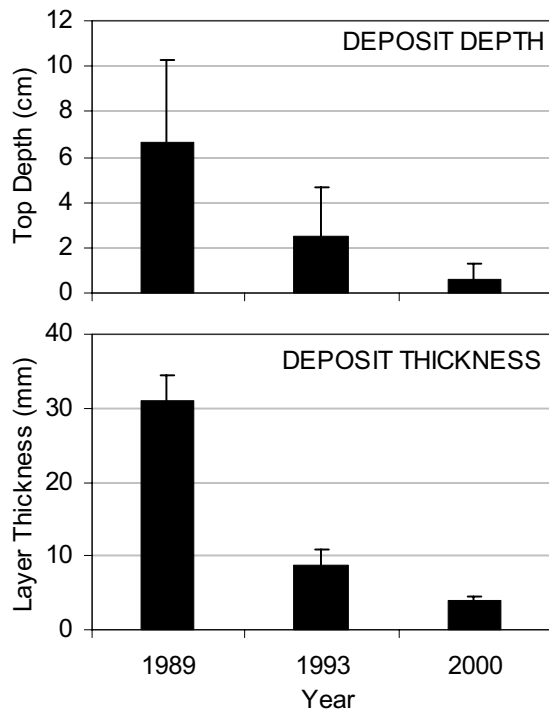


Figure 12. Mean depth to and thickness of sediment deposits associated with overbank flooding in 1989, 1993, and 2000 along the Negliq Channel in the Colville Delta, 2003.

proposed road alignment near the Negliq Channel reveal thick accumulations of layered and massive fine-grained sediments (silt and very fine sand) (Figure 13). Mean ice contents in the three profiles ranged from 60–90%, indicating soils are very ice-rich due to the formation of segregated ice associated with the fine-grained sediments.

Estimates of mean depths of potential thaw settlement ranged from 83–114 cm, based on the assumption that the depth of the active layer would increase to 80–110 cm following severe disturbance (Figure 14). This amount of thaw settlement potentially could lead to impoundment of deep water, which would further increase soil heat flux, and eventually lead to pond development and expansion. Thus, soil properties on the Colville Delta are much more sensitive to disturbance than on the adjacent coastal plain in the NPRA, where estimates of potential thaw settlement ranged from 50 to 76 cm for

alluvial-marine deposits and substantially less for lake basin deposits (Jorgenson et al. 2002).

#### RIVERBANK EROSION

The mean rate of riverbank erosion on the west bank of the Negliq Channel near the proposed road alignment was 0.44 m/yr (SD  $\pm$  0.08,  $n$  = 10) over a 46 year period, based on photogrammetric analysis of 1955 and 2001 airphotos (Figure 15). The maximum rate at any location along the west bank was 0.58 m/yr. On the east bank, however, the vegetated bank accreted at a rate of 0.66 m/y (SD  $\pm$  32,  $n$  = 10) due to the deposition of sediment along a lateral bar.

#### ICE-WEDGE DEGRADATION

The degradation of ice wedges was evaluated across three scales using both field and remote sensing techniques. At the microsite scale, field surveys in 2002 and 2003 examined ice wedges at several bank exposures to assess potential for thermokarst, and sampled 43 locations to assess changes in microtopography, hydrology, soils, and vegetation associated with ice-wedge degradation. At the site scale, thermokarst pits were delineated and classified on photography from 1945, 1982, and 2001 to assess temporal changes in thermokarst development. At the landscape scale, spectral analyses were performed on the 1945 and 2001 photography to assess the extent of ice-wedge degradation in relation to surface geomorphology.

#### FIELD SURVEYS OF MICROSITE CHANGES

Ice wedges in old upland terrain (alluvial-marine deposits, old alluvial terraces) typically were 2.5–3 m across at the top (Figure 16). Lengths of the ice-wedges were not determined, but we estimated the wedges were 3–4 m in length. The ice wedges were capped by 35–45 cm of organic and mineral soil. The active layer above the wedges typically was 30–40 cm, leaving 5–10 cm of frozen soil above the wedge ice. We estimate the wedges are at least 3,000 years old based on rates of wedge development quantified for the Colville Delta (Jorgenson et al. 1997a) and because the upland surfaces have been stable for ~8–10 thousand years based on radiocarbon dating of basal peat layers (Jorgenson et al. 2003a). Based on the stratigraphy at these exposures and the estimated age of the ice, we

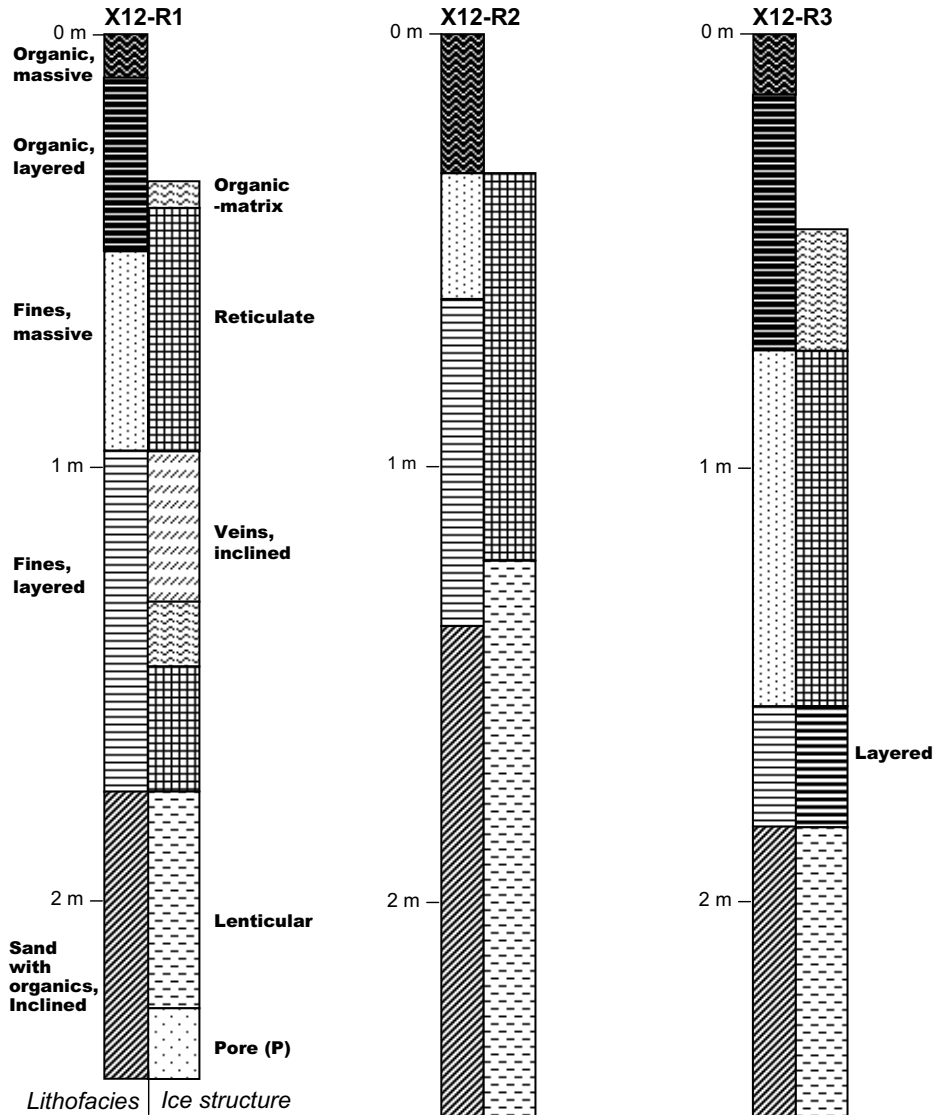


Figure 13. Soil and ice stratigraphy of three cores obtained along the proposed road alignment across the Nigliq Channel, western Colville Delta, 2003.

expect that ice wedges can remain stable under modest thermal changes because of the additional soil that can be incorporated into the active layer to protect the ice wedges if thawing increases slightly. There is, however, only a limited ability to readjust to large thermal changes or surface disturbance before the thawing front encounters wedge ice and degradation and thaw settlement is initiated.

Surface indicators of degrading ice wedges included: (1) deepening troughs and the presence of lateral surface cracks indicating slumping of material into the troughs; (2) ponding of water; (3) health of tussocks ranging from increased

greenness in shallow troughs, indicating an enhanced nutrient regime, to presence of recently killed tussocks in flooded troughs; and (3) changes in vegetation type and composition. Based on these differences we differentiated six stages of ice-wedge degradation: (1) *undegraded* shallow troughs or even surface with no evident changes; (2) *initial degradation* with barely evident settlement and slightly greening of tussocks; (3) *intermediate degradation* with obvious settlement, shallow standing water, and robust green tussocks; (4) *advanced degradation* with deep water-filled pits and dead submerged tussocks; (5) *initial*

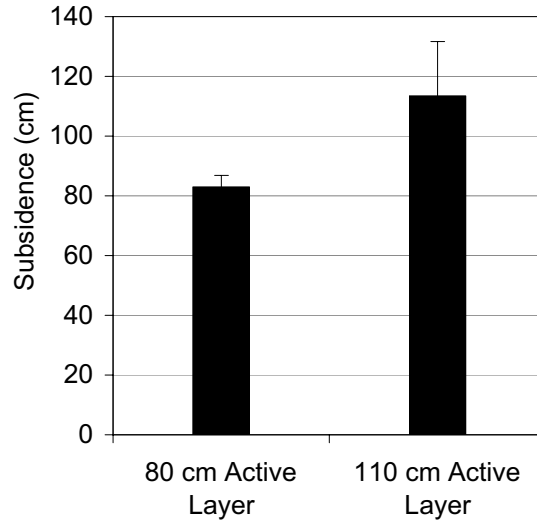


Figure 14. Potential mean ( $\pm$  SD,  $n = 3$ ) thaw settlement estimates for delta inactive floodplain deposits if the active layer increased to either 80 or 110 cm after severe surface disturbance, Colville Delta, 2003.

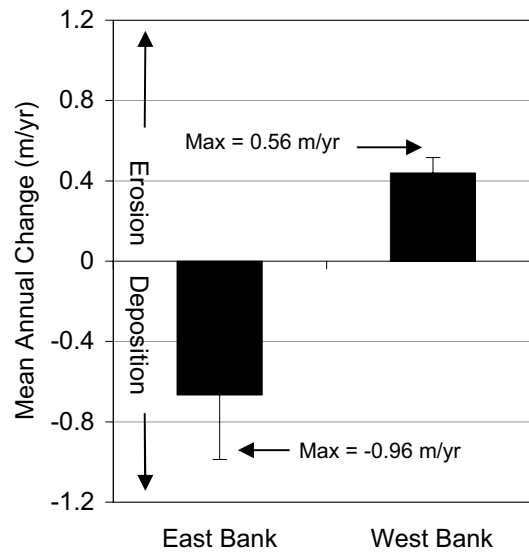


Figure 15. Rates of bank erosion near the proposed road alignment across the Nigliq Channel, western Colville Delta, 2003.



Figure 16. Views of ice wedges at bank exposures illustrating the thin layer of organic and mineral material over massive ice, and sediment deformation between ice wedges, Northeast Planning Area, NPRA, 2003.

Table 1. Characteristics of six stages of ice-wedge degradation in Northeast Planning Area, NPRA, Alaska, 2003.

Stage	Trough Settlement	Surface Water	Vegetation Type	Tussocks	Vegetation Composition
Undegraded Ice Wedges	None	None	Tussock Tundra	Normal	<i>Eriophorum vaginatum</i> , <i>Betula nana</i> , <i>Salix planifolia</i> , <i>Vaccinium vitis idaea</i> , <i>Ledum decumbens</i> , and mosses.
Initial Degradation	Barely evident	None	Tussock Tundra	Somewhat robust	<i>Eriophorum vaginatum</i> , <i>Betula nana</i> , <i>Salix planifolia</i> , <i>Vaccinium vitis idaea</i> , <i>Ledum decumbens</i> , and mosses.
Intermediate Degradation	Shallow	Shallow	Tussock Tundra	Very robust, dark green	<i>Eriophorum vaginatum</i> and <i>Salix planifolia</i> only.
Advanced Degradation	Deep	Deep	Water	Dead, submerged	Trace <i>S. planifolia</i> , <i>Eriophorum angustifolium</i> , <i>Carex aquatilis</i> , and <i>Arctophila fulva</i> .
Initial Stabilization	Moderately Deep	Shallow	Aquatic Sedge Marsh	Dead, buried	<i>Carex aquatilis</i> , <i>E. angustifolium</i> , <i>Caltha palustris</i> , and <i>Calliergon</i> spp.
Advanced Stabilization	Shallow	Shallow to None	Wet Sedge Meadow	Dead, buried	<i>Carex aquatilis</i> , <i>E. angustifolium</i> , <i>E. russeolum</i> , <i>S. planifolia</i> , and <i>Sphagnum</i> spp.

*stabilization* with robust aquatic sedges in shallow water; and (6) *advanced stabilization* with sedges and mosses with water slightly above or below the ground surface (Table 1, Figures 17 and 18)

Surface and soil core measurements that span the entire chronological sequence of thermokarst development revealed that cyclical-type changes occur in trough morphology, water depth and extent, and thaw depth over time. This process begins in the undegraded trough stage and continues to the advanced degradation stage before rebounding to more stable conditions in the advanced stabilization stage (Figure 19). Mean trough depth increased from 5 cm in undegraded troughs to 65 cm (maximum 120 cm) for advanced degradation before decreasing to 29 cm during advanced stabilization. Mean water depth increased from -27 cm below the surface in undegraded troughs to 37 cm above the surface during advanced degradation, and then decreased to 4 cm above the surface during advanced stabilization. Mean thaw depths had smaller changes, increasing from 27 cm in undegraded troughs to 38 cm during intermediate degradation, and then decreasing to 34 cm during advanced

*stabilization*. Thaw depths, however, were measured in early August when thawing had not yet reached maximum depths. In particular, we estimate that thawing beneath the water at the advanced degradation stage likely continued until mid-late September and probably thawed the remaining frozen soil above the wedge ice.

The accumulation of material in the degrading troughs ultimately halts ice wedge degradation. Both the depth of sedge peat on top of degrading tussocks and the depth to wedge ice increased during late stages of development, resulting in the stabilization of the underlying ice wedge. Sedge peat (mostly *Carex aquatilis*) at the surface was absent during the degradation stages and then accumulated rapidly to a mean thickness of 16 cm during advanced stabilization (Figure 19). Mean depth to wedge ice (vertically stratified, opaque ice usually without soil inclusions) increased consistently from 35–58 cm across the degradation sequence.

Finally, ice structures in the frozen soil above the wedge ice changed radically between degradation and subsequent stabilization (Figures 18 and 19). During the undegraded and



Figure 17. Ground views of six stages of ice-wedge degradation. Stages are: undegraded troughs (upper right), initial (upper left), intermediate (middle left), and advanced degradation (middle right), initial (lower left), and advance stabilization (lower right). Northeast Planning Area, NPRA, 2003.

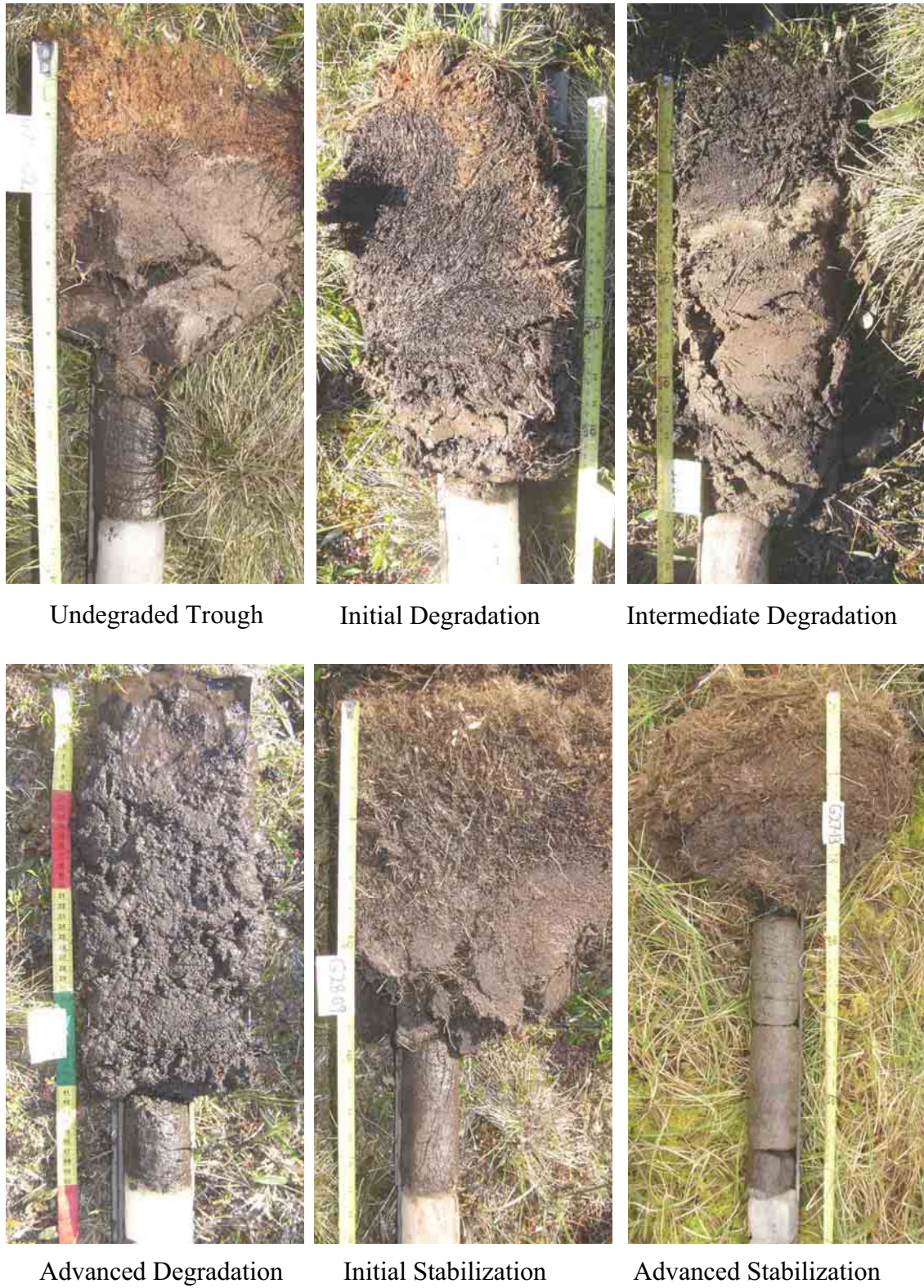


Figure 18. Photographs of soil profiles illustrating changes in soil stratigraphy and ice structures associated with six stages of ice-wedge degradation, Northeast Planning Area, NPRA, 2003.

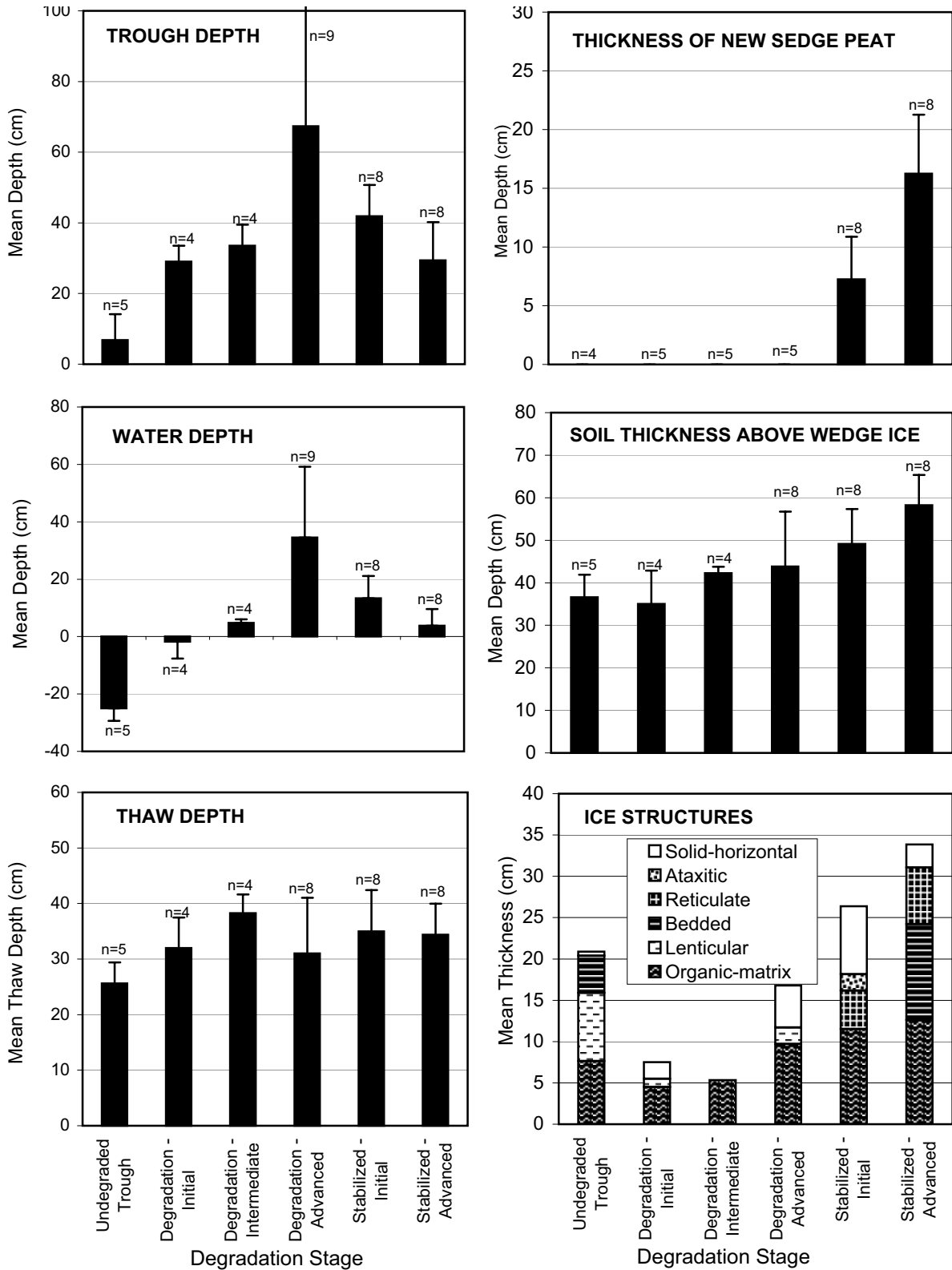


Figure 19. Changes in mean ( $\pm$  SD) trough depths, water depths (negative indicates water is below surface), thaw depths, thickness of new sedge peat, thickness of soil above wedge ice, and thickness of various ice structures associated with six stages of ice-wedge degradation, Northeast Planning Area, NPRA, 2003.

initial-degradation stages, the frozen soil had mostly fine, wavy lenticular ice, with lesser amounts of medium thick (3–5 mm) layered ice and organic-matrix ice. During advanced degradation, the frozen soil had mostly organic-matrix ice, while new solid ice (horizontal oriented transparent ice with small amounts of soil inclusions; also referred to as congelation ice) developed as a thin layer and aggraded to 8 cm during initial stabilization. The thickness of the new ice was highly variable, however, indicating the sensitivity of the aggradation process to site-specific conditions. The new ice presumably formed during rapid freezeback because water is readily available to move to the upward freezing front through the disrupted soils. Finally, during advanced stabilization more complex ice structures developed, including reticulate and layered ice. The reticulate ice presumably developed in response to slow adjustment and thinning of the active layer as new sedge peat accumulated at the surface. The bedded ice presumably developed in response to rapid freezeback in the fall after particular seasonal thawing events.

This evidence indicates that the ice-wedge degradation that we observed is a recent phenomenon and that the ground surface was for the most part stable (allowing readjustment to minor changes) for at least 100s of years and probably 1000s of years prior to the recent degradation. Of particular interest in the degradation sequence was the occurrence of recently drowned tussocks in nearly all of the troughs that we examined. Tussocks can be centuries old (Fetcher and Shaver 1983) and typically develop on surfaces that are at least 1500 yrs old (Jorgenson et al. 1998). Similarly, formation of large ice wedges takes 1500–3000 years (Jorgenson et al. 1998) and the presence of wedge ice near the surface during initial degradation indicates that the surface was relatively stable during the period of ice wedge growth.

Also surprising was the rate at which the degrading troughs became stabilized through the vigorous growth of sedges and rapid accumulation of new sedge peat and that the wedges only partially degrade. Some of the wedges that were in the initial degradation stage after 1982 had progressed to the initial stabilization stage by 2001,

indicating that the development from initial degradation to initial stabilization can occur within 20 years. Once peat starts accumulating above the degraded wedges the stabilization appears irreversible and we expect that the stabilized wedges are unlikely to be able to degrade again without large increases in soil temperature. By the advanced stabilization stage, mean soil thickness above the wedges reaches 58 cm with only 34 cm of seasonal thaw, leaving a protective layer that is nearly double that of undegraded troughs. As evidence of this, pits identified as being in the advanced stabilization stage in 1945 showed little to no change by 2003.

#### PHOTOINTERPRETATION OF DEGRADATION STAGES

Photointerpretation of ice-wedge degradation within two small areas on 1945, 1982, and 2001 airphotos revealed notable changes in the extent and nature of the degradation among years (Figures 20 and 21). The percent of the area (both areas combined, 12.5 ha) covered by degrading and stabilizing thermokarst pits larger than 12 m<sup>2</sup>, which was the minimum size of mappable pits in 1982 and thus basis for standard comparison, increased slowly from 2.1% in 1945 to 2.8% in 1982 and then increased abruptly to 7.4% in 2001. When all pits were included, area increased slowly from 2.2% in 1945 to 2.9% in 1982, and then to 8.6% in 2001, revealing that more pits could be delineated on the larger-scale photography in 2001.

When evaluated by degradation stage, the area of large pits at the advanced-degradation stage increased slowly from 0.5% in 1945 to 0.6% in 1982 and then increased abruptly to 4.4% in 2001. The initial-stabilization stage showed a marked decrease from 0.8% in 1945, to 0.3%, and 0.1% in 1982 and 2001, respectively. In contrast, the advanced-stabilization stage increased continuously from 0.7% to 1.8%, and to 3.0% over the three periods. Finally, the percent area of low basins was 1.2% in 1945 and 1.2% in 1982, but these basins became drained by adjacent thermokarst pits and the subsequent drained basins covered 1.3% in 2001.

These changes reveal how dynamic the tundra surface can be over relatively short periods. First, there has been an abrupt increase in ice-wedge degradation since 1982. Second, the areas that

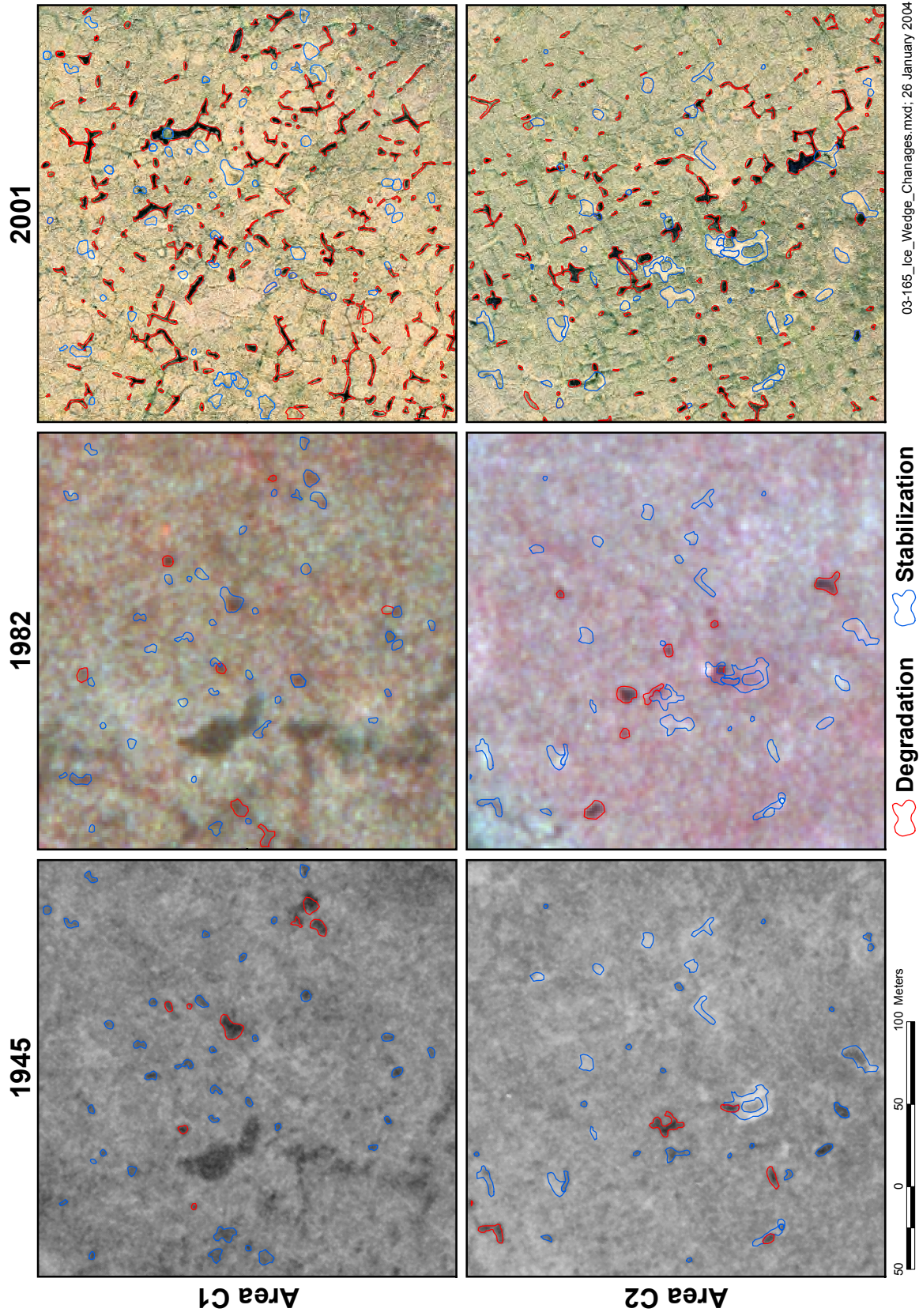


Figure 20. Abundance of thermokarst pits on airphotos taken in 1945, 1982, and 2001 within two 250 × 250 m areas, Northeast Planning Area, NPRA, 2003..

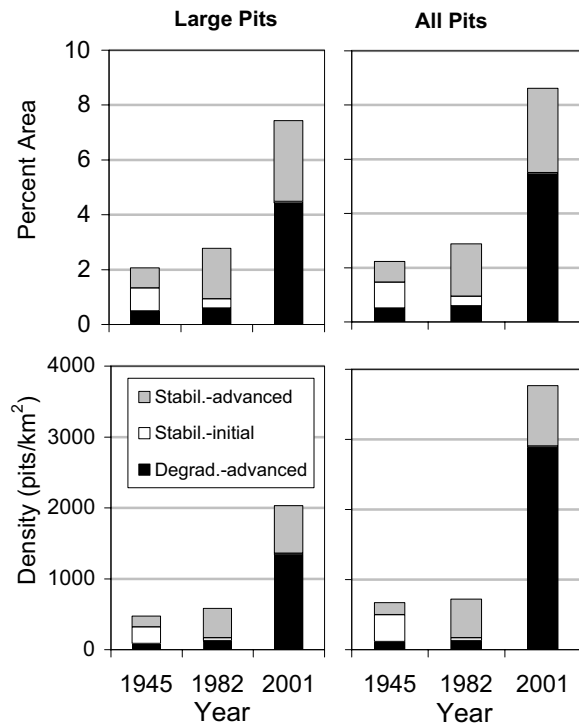


Figure 21. Percent area and density of thermokarst pits associated with ice-wedge degradation evident on airphotos taken in 1945, 1982, and 2001 for two small map areas (6.25 ha), Northeast Planning Area, NPRA, 2003. Comparisons are presented for only large ( $>12 \text{ m}^2$ ) pits, which are consistently evident across all scales of airphotos, and for all pits, which more completely enumerates the degradation evident on the large-scale airphotos from 2001.

reached advanced degradation become stabilized relatively quickly; pits that were in the advanced degradation stage in both 1945 and 1982 changed to the initial or advanced stabilization stages by the subsequent photo period. Third, the small amount (0.8%) of pits in the initial-stabilization stage in 1945 indicates that a small amount of degradation probably occurred shortly before 1945.

#### SPECTRAL ANALYSIS OF EXTENT OF DEGRADATION

Spectral classification of water was used as an indirect measure of changes in the abundance of ice wedges in the advanced degradation stage, which is characterized by having water that typically is 15–120 cm deep (Figures 22 and 23).

The analysis of small waterbodies in the terrestrial portion (excluding permanent deep lakes and ponds covering 20.2 % of the total area) of the central map area (1450-ha areas) showed 14.1% of the area was flooded only in 1945, 3.5% was flooded only in 2001, and 1.9% in both years (Figure 24). In the western map area (excluding 30% covered by large waterbodies), 13.2% of the terrestrial terrain was flooded only in 1945, 4.3% was flooded only in 2001, and 2.5% in both years. Over both areas, flooding covered 13.7% of the terrestrial area in 1945 only, 3.8% in 2001 only, and 2.2% in both years. Because 2001 was much drier than 1945, we attribute the development of new waterbodies in 2001 to be due to ice-wedge degradation.

When the areal extent of flooding was analyzed by terrain unit and then grouped by upland and lowland terrain, we found a distinct separation between the two groups in the central and western map areas (Figure 24). In upland areas, flooding of alluvial-marine deposits and the domed ice-rich centers of drained basins was much less than for the margins of ice-rich and ice-poor basins in low-lying areas. When both map areas were combined, the extent of flooding in upland areas was 1.7% in 1945 only, 4.3% in 2001 only, and 0.1% in both years. In lowland areas, flooding covered 16.2% of the terrestrial area in 1945 only, 3.5% in 2001 only, and 2.7% in both years. This distinction between upland and lowland physiography allows a reliable interpretation of ice wedge degradation associated with the 4.3% increase in small waterbodies in 2001, whereas, the interpretation of waterbody changes in wet lowland areas is less certain. This increase in waterbodies in 2001 and the redistribution of water from round, low polygonal basins into small linear troughs is consistent with the more detailed time-series analysis derived from manual photointerpretation.

The waterbody analysis provides only a minimum estimate, however, because ground observations indicated that many polygonal troughs over ice-wedges had indications of subsidence, yet were not sufficiently low to be covered by water. Consequently, the initial and intermediate stages of degradation were not distinct enough to be mapped on 1945 and 1982 small-scale photography. Assuming that ice wedges occupy 10–20% of the volume of

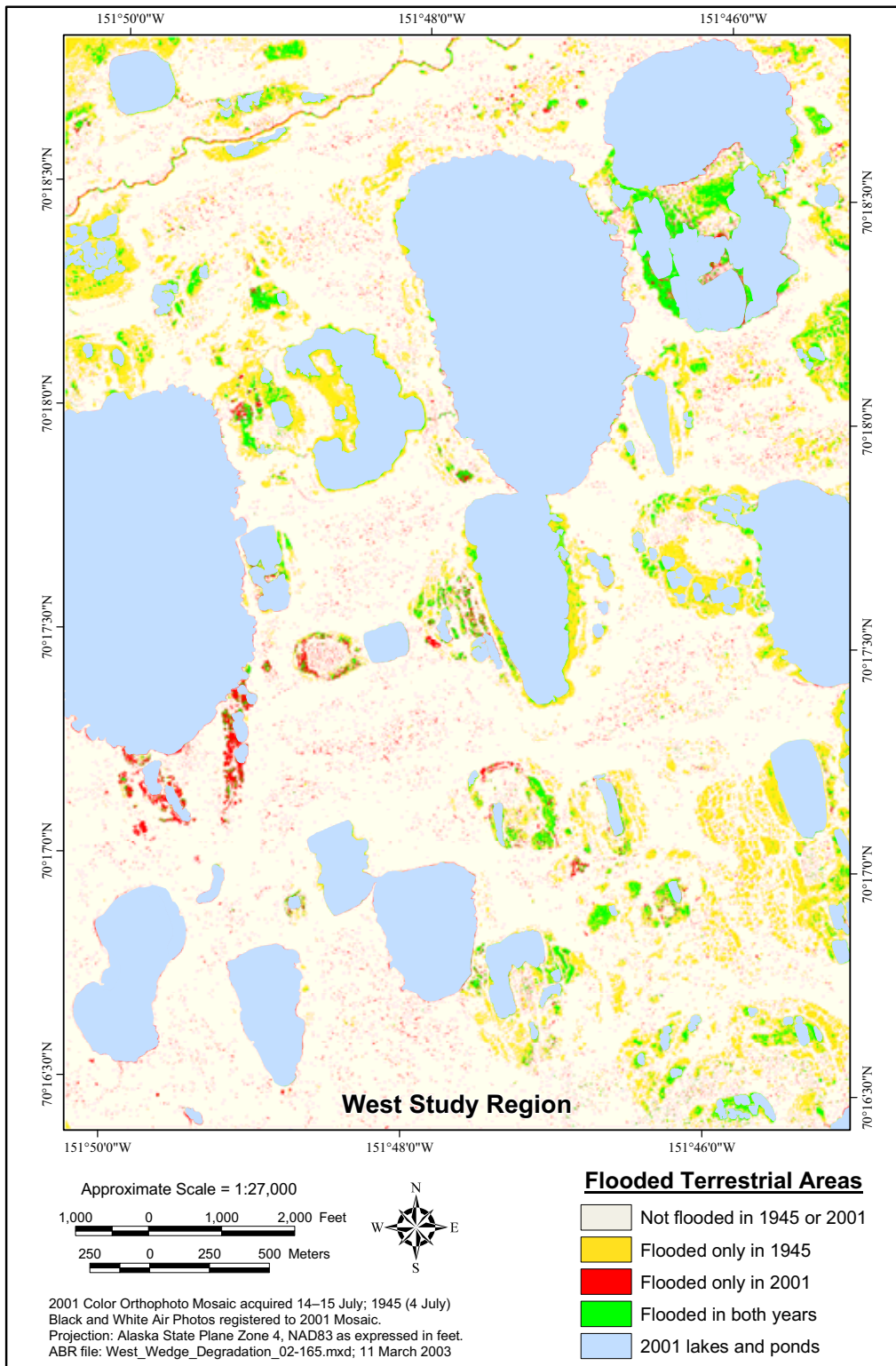


Figure 22. Changes in flooded areas in the west change study region 1945 and 2001 used to differentiate areas of thermokarst, Northeast Planning Area, NPRA, 2003. Small waterbodies (red) present only in 2001 are attributed to thermokarst.

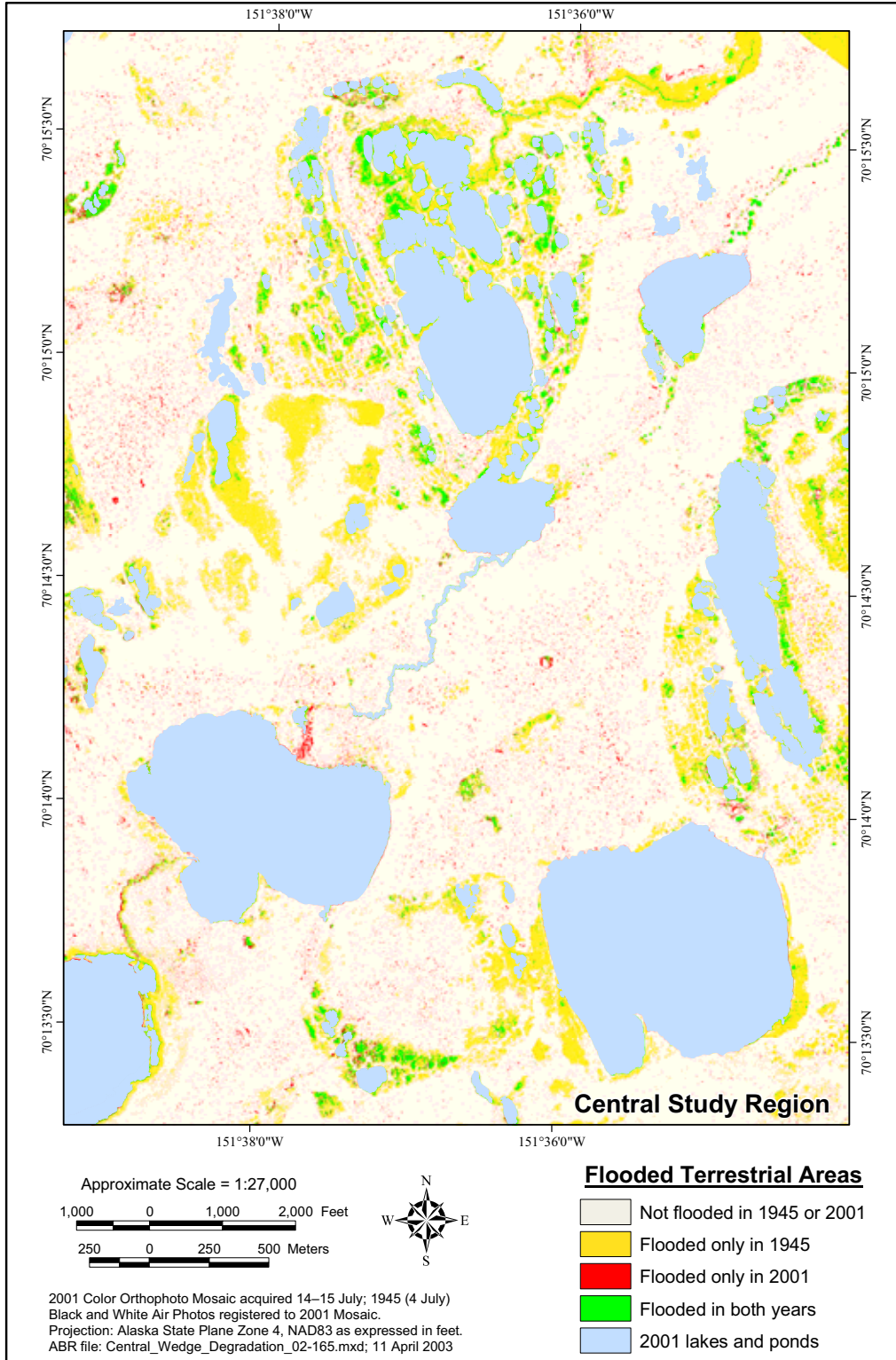


Figure 23. Changes in flooded areas in the central change study region between 1945 and 2001 used to differentiate areas of thermokarst, Northeast Planning Area, NPRA, 2003. Small waterbodies (red) present only in 2001 are attributed to thermokarst.

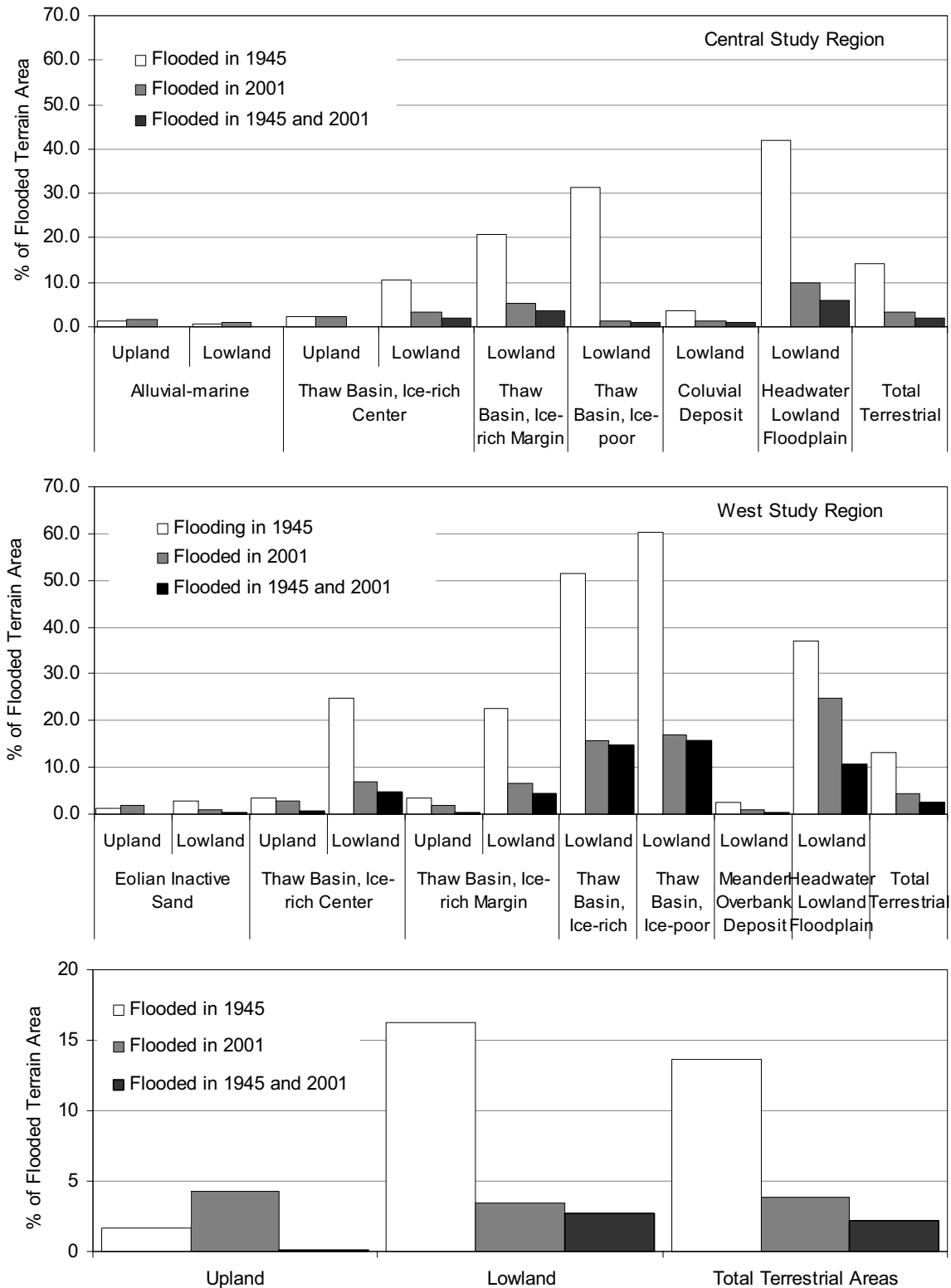


Figure 24. Summary of changes in flooded areas between 1945 and 2001 by terrain unit and physiography for the central and western map areas, Northeast Planning Area, NPRA, 2003.

near-surface terrestrial deposits, the analysis indicates that at least 20–40% of the ice wedges have undergone partial degradation.

#### FACTORS AFFECTING DEGRADATION

We attribute the recent, abrupt degradation of ice wedges to warm temperatures during 1989–1998. Climatic records for Barrow indicate that mean annual temperatures were substantially warmer in 1989 (-10.2 °C), 1993 (-10.2 °C), and 1995–1998 (-8.4 to -10.9 °C) than the long-term (1921–2002) average (-12.3 °C). Indeed, four of the five highest mean annual temperatures in the historical record occurred during this period (Figure 25). On a decadal basis, the ten-year running average had an initial peak of -11.2 °C centered around 1939, decreased during the mid-1950s to mid-1970s to a low of -13.2 °C around 1973, and increased to -10.5 °C around 1997. Thus, the ten-year running average indicates a general warming trend of nearly 2°C from the mid-1970s to the 1990s. Similarly, permafrost temperatures measured on the Arctic Coastal Plain near Prudhoe Bay indicate that permafrost has warmed by 2–3 °C since the mid-1980's (Romanovsky and Osterkamp 1997, Osterkamp 2003). Over the whole recorded period, however, regression analysis indicates mean annual air temperatures have only increased at a rate of 0.6 °C/80 yr (1921–2002). Based on qualitative examination of other aerial photography obtained in 1979 (this area) and 1984 (Kuparuk oilfield) that lacked the prominent waterbodies along the ice-wedge polygon network and the substantial increase in recent air and ground temperatures, we conclude that most of the degradation we have observed occurred during 1989–1998, when mean annual air temperatures were frequently 2–4 °C above the long-term average. That ice wedges can degrade even in cold permafrost where mean annual temperatures are around -7 to 11°C is remarkable.

Our analyses also have revealed that ice-wedge degradation has resulted in a substantial redistribution of surface water from the centers of low-centered polygon to the adjacent degraded trough network. This redistribution of water and lowering of the water table has important implications for plant community changes, soil respiration, and release of trace gases.

Understanding this natural process of thermokarst development is useful in assessing the rates of human-induced thermokarst and ultimate stabilization, assessing the relative impacts of human-induced thermokarst during oilfield development, and for developing land rehabilitation plans that compensate for microtopographic and hydrologic changes associated with thaw settlement.

#### SUMMARY AND CONCLUSIONS

Permafrost greatly influences the engineering properties of the soil, ecosystem development, and the response of the terrain to human activities. Accordingly, the study of terrain relationships for predicting the nature and distribution of ground ice across the landscape, and the evaluation of how permafrost will respond to disturbance is essential to assessing potential impacts from oil development in the National Petroleum Reserve–Alaska (NPR). This third year of permafrost studies in northeastern NPR was designed to (1) determine the nature and abundance of ground ice at multiple spatial scales to develop terrain relationships for predicting ice distribution, (2) assess flood sedimentation, permafrost characteristics, and riverbank erosion along the proposed road alignment on the floodplain of the western Colville Delta, and (3) assess the rates of landscape change associated with ice-wedge degradation.

#### FLOODPLAIN DEVELOPMENT ON FISH AND JUDY CREEKS

Changes in elevation, soils, surface-forms, and vegetation were surveyed across two toposequences along Fish Creek and one toposequence along Judy Creek, areas that are of interest for oil spill contingency planning and potentially could be of interest for oil development in the future. These toposequences are a surrogate for evaluating changes over time and thus provide a record of terrain development on the meandering floodplains.

Active channel deposits were dominated by inclined or rippled fine to medium sands, indicating frequent scouring and deposition. Soil pH ranged from 7.4–8.2, electrical conductivity (EC) from 20–130 µS/cm and ice volume from

30.7–47.3% (mean 37%), within the 2.5 m coring depth. Active overbank deposits typically have laminar, interbedded silts and very fine sands, indicating frequent flooding and vertical accretion of sediments. Soil pH ranged from 7.4–8.2, EC from 10–220  $\mu\text{S}/\text{cm}$ , and ice volume from 12–59% (mean = 37%). Inactive overbank deposits typically had interbedded organic and very fine sand and silt horizons, indicative of infrequent flooding and sedimentation. Soil pH ranged from 6.2–8.3, EC from 40–910  $\mu\text{S}/\text{cm}$ , and ice volume from 38.1–72.7% (mean = 55%). Abandoned floodplain cover deposits had thick accumulations of peat at the surface underlain by interbedded sands and organics, indicating flooding is rare. Soil pH ranged from 4.7–6.9, EC from 100–570  $\mu\text{S}/\text{cm}$ , and ice volume from 64–100% (mean = 78%). Finally eolian active and inactive deposits were comprised of massive and inclined sands. Soil pH values ranged from 7.1–8.0, EC from 60–270  $\mu\text{S}/\text{cm}$ , and ice volume from 29.6–43.8% (mean = 40%). Mean accumulation rates were 0.51 mm/yr for one inactive overbank deposit and 0.26 mm/yr for one abandoned overbank deposit, based on radiocarbon dating of basal organic matter at each site. These results reveal large changes during floodplain development associated with changes in flooding and sedimentation: (1) soils change from medium to fine sands to thick organic matter accumulations at the surface, (2) soils are alkaline early on but become increasingly acidic with age, and (3) ice volumes are initially low because of the coarse material, and become high during late stages because of the accumulation of silts and organics.

### **SEDIMENTATION, PERMAFROST, AND BANK EROSION NEAR THE NEGLIQ CHANNEL CROSSING**

Sediment deposition associated with three large flood events was measured along the proposed road alignment crossing the Nigliq Channel in the western Colville Delta during mid-August 2003. Sedimentation from overbank flooding in 1989, 1993, and 2000 created deposits of silt to very fine sand that had mean thicknesses of 30, 9, and 4 mm at mean depths of 6.6, 2.5, and 0.6 cm, respectively. The estimated return intervals for these three floods are ~5, ~20, and 100

years, respectively. The deposition of thin deposits during infrequent floods and thick deposits during rare floods has ecological importance for sustaining relatively high productivity on floodplain environments. The thin deposits are insufficient to damage vegetation but do contribute periodic nutrient inputs bound to the sediments. In contrast, thick deposits from large floods can smother vegetation, particularly close to the riverbank. While shrubs incur little to no damage, and much of the herbaceous vegetation can resprout through the sediment, mosses and lichens are killed.

Permafrost samples from three cores on the inactive floodplain adjacent to the proposed road alignment near the Nigliq Channel indicate soils are very ice-rich. The profiles reveal thick accumulations of layered and massive fine-grained sediments (silt and very fine sand) that are particularly susceptible to ice segregation. Mean ice contents in the three profiles ranged from 60–90%. Mean depths of potential thaw settlement ranged from 83–114 cm, based on the assumption that the active layer would increase to depths of 80–110 cm after severe disturbance. These conditions are much more sensitive to disturbance than the terrain units found in the adjacent coastal plain in the NPRA, where estimates of potential thaw settlement ranged from 50–76 cm for alluvial-marine deposits and substantially less for lake basin deposits (< 35 cm).

The mean rate of riverbank erosion along the Nigliq Channel near the proposed road alignment was 0.44 m/yr (SD  $\pm$  0.08,  $n = 10$ ) on the west bank over a 46 year period, based on photogrammetric analysis of 1955 and 2001 airphotos. The maximum rate at any location along the west bank was 0.58 m/yr. On the east bank, however, the vegetated bank accreted at a rate of 0.66 m/y (SD  $\pm$  32,  $n = 10$ ) due to the deposition of sediment along the lateral bar. This information can be incorporated into the future design of potential river crossing structures.

### **ICE WEDGE DEGRADATION**

The degradation of ice wedges was evaluated across three scales using both field and remote sensing techniques and included: (1) field sampling at 43 locations to assess vegetative,

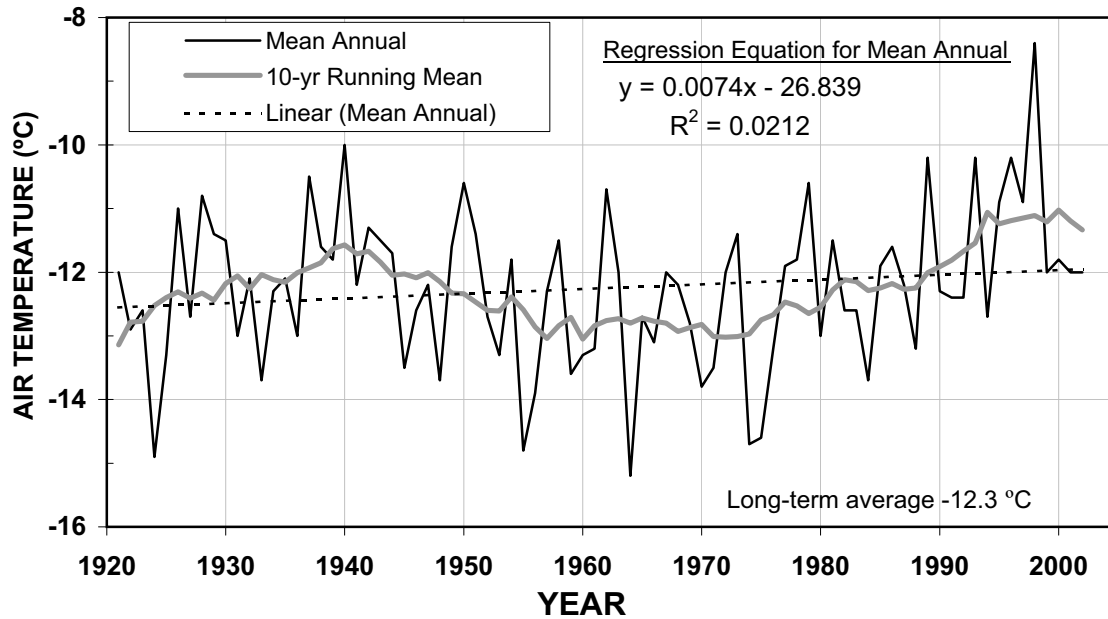


Figure 25. Mean annual air temperatures for Barrow Alaska, 1921–2003.

microtopographic, and soil indicators of ice-wedge degradation at the microsite scale; (2) delineation and classification of thermokarst pits on photography from 1945, 1982, and 2001 to assess temporal changes in thermokarst development at the site scale, and (3) spectral analysis of 1945 and 2001 photography to assess the extent of ice-wedge degradation in relation to surface geomorphology at the landscape scale.

Ice wedges in old upland terrain (alluvial-marine deposit, old alluvial terrace) typically were 2.5–3 m across at the top, 3–4 m deep and capped by 35–45 cm of organic and mineral soil. This high volume of ice and thin soil cover create conditions that are sensitive to climatic change and surface disturbance. Ice-wedge degradation sampled at 43 locations was differentiated into six stages based on changes in trough depth, water depth, soil stratigraphy, and vegetation. These include: (1) undegraded troughs with no evident changes; (2) initial degradation with barely evident settlement and slightly greening of tussocks; (3) intermediate degradation obvious settlement, shallow standing water, and robust green tussocks; (4) advanced degradation with deep water filled pits and dead submerged tussocks; (5) initial stabilization with robust aquatic sedges in shallow water; and (6) advanced stabilization with sedges in mosses with water

slightly above or below the ground surface. The progression from initial degradation through advanced degradation and finally to advanced stabilization was accompanied by large changes in mean trough depths (5, 65, and 29 cm respectively), mean water depths (-27, 37, and 4 cm), mean thaw depths (27, 38, and 34 cm), mean depth to wedge ice (35, 44, and 58 cm), mean thickness of new sedge peat (0, 0, and 16 cm), and mean thickness of frozen soil over the ice wedges (8, 17, and 34 cm).

Photointerpretation of ice-wedge degradation within two small areas on 1945, 1982, and 2001 airphotos revealed notable changes in the extent and nature of the degradation among years. The percent of the area (both areas combined, 12.5 ha) covered by degrading and stabilizing thermokarst pits larger than 12 m<sup>2</sup>, which was the minimum size of mappable pits in 1982 and thus basis for standard comparison, increased slowly from 2.1% in 1945 to 2.9% in 1982 and then increased abruptly to 7.4% in 2001. When evaluated by degradation stage, the area of large pits in the advanced-degradation stage increased slowly from 0.5% in 1945 to 0.6% in 1982 and then increased abruptly to 4.4% in 2001. The initial-stabilization stage showed a marked decrease from 0.8% in 1945, to 0.3%, and 0.1% in 1982 and 2001, respectively. In contrast, the

advanced-stabilization stage increased continuously from 0.7% to 1.8%, and to 3.0% over the three periods. Finally, the percent area of low basins was 1.2% in 1945 and 1.2% in 1982, but these basins became drained by adjacent thermokarst pits and the subsequent drained basins covered 1.3% in 2001. These changes reveal how dynamic the tundra surface can be over relatively short periods and highlight several important processes: (1) there has been an abrupt increase in ice-wedge degradation since 1982, and (2) areas that reach the advanced degradation stage become stabilized relatively quickly and undergo little change thereafter.

Spectral analysis of waterbody characteristics over a broader area (29 km<sup>2</sup>) revealed flooding covered 13.7% of the terrestrial area (larger waterbodies excluded) in 1945 only, 3.8% in 2001 only, and 2.2% in both years. We attributed the increase in newly flooded areas (3.8%) in 2001 (a dry year) not present in 1945 (wet year) to be the result of thermokarst. The low percent of areas flooded in both years indicates the thermokarst has resulted in a redistribution of water from round flooded polygon centers to linear degrading troughs.

This evidence indicates that the thermokarst we observed is a recent phenomenon. The prevalence of dead tussocks, which can be centuries old, indicates that the ground surface has been stable for 100s of years before this recent degradation. The presence of large ice wedges, which take 1500–3000 years to develop, and the lack of thick sedge peat and complex ice structures that form over wedges that have previously degraded and stabilized during initial degradation stages that we sampled, indicate that the wedges probably were stable for 1000s years prior to the recent degradation. We attribute the recent degradation to warm temperatures that occurred during 1989–1998. Climatic records for Barrow indicate that mean annual temperatures were substantially warmer in 1989 (-10.2 °C), 1993 (-10.2 °C), and 1995–1998 (-8.4 to -10.9 °C) than the long-term (1921–2002) average (-12.3 °C). Similarly, permafrost temperatures near Prudhoe Bay indicate that permafrost has warmed by 2–3 °C since the mid-1980's. This recent degradation has caused a substantial redistribution of surface water from the centers of low-centered polygon to the

adjacent trough network. Understanding of these natural processes are useful in assessing the rates of human-induced thermokarst and ultimate stabilization and for developing land rehabilitation plans that compensate for microtopography and hydrologic changes associated with thaw settlement.

#### LITERATURE CITED

- Billings, W. D., and K. M. Peterson. 1980. Vegetational change and ice-wedge polygons through the thaw lake cycle in Arctic Alaska. *Arctic and Alpine Research* 12: 413–432.
- Britton, M. E. 1957. Vegetation of the Arctic tundra. Pages 67–113 in H. P. Hansen, ed. *Arctic Biology: 18th Biology Colloquium*. Oregon State University Press, Corvallis.
- Brown, J. 1968. An estimation of the volume of ground ice, Coastal Plain, Northern Alaska. U. S. Army Cold Regions Research and Engineering Laboratory, Hanover, NH.
- Brown, J., and N. A. Grave. 1979. Physical and thermal disturbance and protection of permafrost. U.S. Army Cold Regions Research and Engineering Laboratory, Hanover, NH. Special Report 79-5. 42 pp.
- Burgess, R. M., E. R. Pullman, and M. T. Jorgenson. 1998. Evaluation of vertical migration of salts from buried reserve pit materials in the Kuparuk and Prudhoe Bay oilfields. Final report prepared for Arco Alaska, Inc., Anchorage, by ABR, Inc., Fairbanks, AK. 55 + appendices pp.
- Burgess, R. M., E. R. Pullman, T. C. Cater, and M. T. Jorgenson. 1999. Rehabilitation of salt-affected land after close-out of reserve pits. Third Annual Report prepared for ARCO Alaska, Inc., Anchorage, AK, by ABR, Inc., Fairbanks, AK. 48 pp.
- Carter, L. D., J. A. Heginbottom, and M. Woo. 1987. Arctic Lowlands. Pages 583–628 in *Geomorphic Systems of North America*. Centennial Special Volume, 2 ed., U.S. Geological Society of America, Boulder, CO.

- Emers, M., and J. C. Jorgenson. 1997. Effects of winter seismic exploration on tundra vegetation and the soil thermal regime on the Arctic National Wildlife Refuge, Alaska. Pages 443-456 in R. M. M. Crawford, ed. *Disturbance and Recovery in Arctic Lands, An Ecological Perspective*. Kluwer Academic Publishers, Dordrecht, Netherlands.
- Fetcher, N. and Shaver, G. R. 1982. Growth and tillering patterns within tussocks of *Eriophorum vaginatum*. *Holarctic Ecology* 5:180-186.
- Hinkel, K. M., F. E. Nelson, Y. Shur, J. Brown, and K. R. Everett. 1996. Temporal changes in moisture content of the active layer and near-surface permafrost at Barrow, Alaska, U.S.A.: 1962–1994. *Arctic and Alpine Research* 28: 300–310.
- Johnson, G. H. 1981. *Permafrost Engineering Design and Construction*. National Research Council of Canada, Ottawa, Canada. 540 pp.
- Jorgenson, M. T. 1986. Biophysical factors affecting the geographic variability of soil heat flux. M.S. Thesis, Univ. of Alaska, Fairbanks, 109 pp.
- Jorgenson, M. T., and J. G. Kidd. 1991. Land rehabilitation studies in the Prudhoe Bay Oilfield, Alaska, 1990. Annual report prepared for ARCO Alaska, Inc., Anchorage, AK, by Alaska Biological Research, Inc., Fairbanks, AK. 57 pp.
- Jorgenson, M. T., J. W. Aldrich, J. G. Kidd, and M. D. Smith. 1993. *Geomorphology and hydrology of the Colville River Delta, Alaska, 1992*. Final Report prepared for ARCO Alaska, Inc., Anchorage, by Alaska Biological Research, Inc., and Arctic Hydrologic Consultants, Fairbanks. 79 pp.
- Jorgenson, M. T., J. W. Aldrich, E. Pullman, S. Ray, M. D. Smith, and Y. Shur. 1996. *Geomorphology and hydrology of the Colville River Delta, Alaska, 1995*. Final report prepared for ARCO Alaska, Inc., Anchorage, by ABR, Inc. and Shannon and Wilson, Inc., Fairbanks.
- Jorgenson, M. T., L. W. Krizan, and M. R. Joyce. 1991. Bioremediation and tundra restoration after an oil spill in the Kuparuk Oilfield, Alaska, 1990. Pages 149-154 in *Proceedings of the 14th Annual Arctic and Marine Oil Spill Technical Program*. Environ. Canada, Ottawa, ON.
- Jorgenson, M. T., E. R. Pullman, T. Zimmer, Y. Shur, A. A. Stickney, and S. Li. 1997a. *Geomorphology and hydrology of the Colville River Delta, Alaska, 1996*. Final report prepared for ARCO Alaska, Inc., Anchorage, AK, by ABR, Inc., Fairbanks, AK. 148 pp.
- Jorgenson, M. T., J. E. Roth, E. R. Pullman, R. M. Burgess, M. Raynolds, A. A. Stickney, M. D. Smith, and T. Zimmer. 1997b. *An ecological land survey for the Colville River Delta, Alaska, 1996*. Final report prepared for ARCO Alaska, Inc., Anchorage, AK, by ABR, Inc., Fairbanks, AK. 160 pp.
- Jorgenson, M. T., Y. Shur, and H. J. Walker. 1998. Factors affecting evolution of a permafrost dominated landscape on the Colville River Delta, northern Alaska. Pages 523-530 in A. G. Lewkowicz, and M. Allard, eds. *Proceedings of Seventh International Permafrost Conference*. Universite Laval, Sainte-Foy, Quebec. Collection Nordicana, No. 57.
- Jorgenson, M. T., E. R. Pullman, and Y. Shur. 2002. *Geomorphology of the NPRA study area, northern Alaska*. Unpublished report prepared for Phillips Alaska, Inc., Anchorage, AK, by ABR, Inc., Fairbanks, AK. 50 pp.
- Jorgenson, M. T., E. R. Pullman, and Y. L. Shur. 2003a. *Geomorphology of the Northeast Planning Area of the National Petroleum Reserve-Alaska, 2002*. Final report prepared for Phillips Alaska, Inc., Anchorage, AK, by ABR, Inc., Fairbanks, AK. 67 pp.
- Jorgenson, M. T.; Roth, J. E.; Emers, M.; Schlentner, S.; Swanson, D. K.; Pullman, E.; Mitchell, J., and Stickney, A. A. 2003b. *An ecological land survey for the Northeast Planning Area of the National Petroleum*

- Reserve – Alaska, 2002. Final Report prepared for ConocoPhillips, Alaska, Inc., Anchorage, AK by ABR, Inc., Fairbanks, AK. 128 pp.
- Kidd, J. G., L. L. Jacobs, T. C. Cater, and M. T. Jorgenson. 1997. Ecological restoration of the North Prudhoe Bay State No. 2 exploratory drill site, Prudhoe Bay Oilfield, Alaska, 1995. Final Report prepared for ARCO Alaska, Inc., Anchorage, AK, by ABR, Inc., Fairbanks, AK. 36 pp.
- Kreig, R. A., and R. D. Reger. 1982. Air-photo analysis and summary of landform soil properties along the route of the Trans-Alaska Pipeline System. Alaska Division of Geological and Geophysical Surveys, Fairbanks, AK. Geologic Report 66. 149 pp.
- Lawson, D. E. 1986. Response of permafrost terrain to disturbance: a synthesis of observations from northern Alaska, U.S.A. *Arctic and Alpine Research* 18: 1–17.
- McFadden, T. T., and F. L. Bennet. 1991. Construction in Cold Regions—A Guide for Planners, Engineers, Contractors, and Managers. John Wiley and Sons, Inc., New York, NY.
- Michael Baker Jr., Inc. 2000. 2000 Colville River Delta spring breakup and hydrologic assessment. Unpubl. Rep. prepared for PHILLIPS ALASKA, Inc., Anchorage.
- Murton, J. B., and H. M. French. 1994. Cryostructures in permafrost, Tuktoyaktuk coastlands, western arctic Canada. *Canadian Journal Earth Science* 31: 737–747.
- Osterkamp, T. E. 2003. A thermal history of permafrost in Alaska. Pages 863–869 in *Proceedings of Eighth International Conference on Permafrost*, Zurich, Switzerland.
- Pollard, W. H., and H. M. French. 1980. A first approximation of the volume of ground ice, Richards Island, Pleistocene Mackenzie Delta, Northwest Territories, Canada. *Canadian Journal of Earth Sciences* 17:509-516.
- Romanovsky, V. E., and T. E. Osterkamp. 1997. Thawing of the active layer on the coastal plain of the Alaska Arctic. *Permafrost and Periglacial Processes* 8.
- Shannon and Wilson, Inc. 1997. Colville River Delta Two-Dimensional Surface Water Model. Annual Report prepared for Michael Baker, Jr., Inc. and ARCO Alaska, Inc., Anchorage, AK, by Shannon and Wilson, Inc., Fairbanks, AK.
- Walker, D. A., K. R. Everett, P. J. Webber, and J. Brown. 1980. Geobotanical atlas of the Prudhoe Bay region, Alaska. U.S. Army Corps of Engineers Cold Regions Research and Engineering, Hanover, NH. Laboratory Report 80-14. 69 p.
- Walker, D. A. 1981. The vegetation and environmental gradients of the Prudhoe Bay region, Alaska. Unpublished report by University of Colorado, Boulder.
- Walker, D. A., D. Cate, J. Brown, and C. Racine. 1987. Disturbance and recovery of arctic Alaskan tundra terrain: a review of investigations. U.S. Army Cold Regions Research and Engineering Laboratory, Hanover, NH. CRREL Rep. 87-11.
- Webber, P. J., and J. D. Ives. 1978. Damage and recovery of tundra vegetation. *Environmental Conservation* 5: 171–182.
- Webber, P. J., P. C. Miller, F. S. Chapin III, and B. H. McCown. 1980. The vegetation: pattern and succession. Pages 186-218 in J. Brown, P. C. Miller, L. L. Tieszen, and F. L. Bunnell, eds. *An arctic ecosystem, the coastal tundra at Barrow, Alaska*. Dowden, Hutchinson, and Ross, Stroudsburg, PA.

Appendix 1. Classification and description of lithofacies observed in North Slope soils, 2003. Structures less <4 in. (10 cm) thick are not broken out.

Lithofacies class (and code)	Primary and secondary particle sizes	Sedimentary structures	Mechanism interpretation
Gravel, massive (Gm)	Clean gravel (little or no fines)	None visible	Longitudinal bars, lag deposits, sieve deposits
Gravels, fine matrix (Gfm)	Gravel supported by fine matrix	None visible,	Debris flow, glacial till,
Gravel, layered (Gl)	Clean grave (some sand layers)	Horizontal layers or crudely stratified gravel	Longitudinal bars, lag deposits, sieve deposits
Gravel-trough crossbeds (Gct)	Clean gravel	Stratified with trough crossbeds	Minor channel fills
Gravel-planar crossbeds (Gcp)	Clean gravel	Stratified with planar crossbeds	Linguoid bars or deltaic growths from older bar remnants
Gravels-gradational (Gg)	Platy, angular, to subangular gravel	Gradational structure, clasts increasing with depth	Residual soil over weathered bedrock
Sands-massive (Sm)	Medium-coarse sands	None visible, medium-coarse, light brown sands, may be pebbly	Uncertain
Sands, massive with trace gravel (Sgm, was Smg)	Medium-coarse sands, loamy sands, with trace gravels.	None visible	Coastal plain, reworked coastal environment from coastal or thaw lake processes
Sands with trace gravel, massive, turbated (Sgmt)	Sands, loamy to fine sands (uncommonly medium sand) with trace gravels.	Turbated, intermixed massive sand and organics inclusions and widely dispersed pebbles	Coastal plain, cryoturbated sediments, problematic origin,
Sand, layered (Sh, was Sl)	Sand, very fine to coarse	Horizontally stratified layers	Planar bed flow (lower and upper flow regime), levees
Sands, inclined (Si)	Sand, very fine to coarse	Undifferentiated wavy-bedded, ripple, or crossbed stratified layers. Interpretation limited by small size of cores.	Lower flow regime and eolian sand
Sands with organics, inclined (Soi)	Fine-medium-coarse sands with interbedded detrital peat layers	Undifferentiated wavy-bedded, ripple, or crossbed structure	Lateral accretion deposits during flood stage in organic-rich landscapes
Sands, rippled (Sr, but use Si unless very distinctive)	Sand, very fine to coarse	Ripples with variable internal structure, typically 3 cm high, 10-15 cm, internally graded,	Lower flow regime
Sands with organics, turbated (Sot)	Very fine to medium sands with organic inclusions	Isolated, deformed organic inclusion with sandy matrix	Coastal plain deposits with cryoturbation or massive thermokarst

Appendix 1. (Continued).

Lithofacies class (and code)	Primary and secondary particle sizes	Sedimentary structures	Mechanism interpretation
Fines, massive (Fm)	Silts and silt loam	None visible	Overbank deposition of sediments or eolian input
Fines with organics, massive (Fom)	Silts and silt loam with well-decomposed organics	None visible,	Soil formation in massive silts
Fines with organics, turbated (Fot)	Silts, silt loam with poorly decomposed organic inclusions	Disrupted organic and mineral inclusions due to cryoturbation	Compression and displacement of material during freezing and thawing, thermokarst
Fines, layered (Fl)	Silts and fine sands	Horizontally stratified layers	Proximal overbank deposition of sediments
Fines with clay, massive (Fcm, was Fsc)	Clay-rich silts and fine sands	None visible to indistinct lamination	Lacustrine,
Fines with clay, laminar (Fcl, was Flc)	Clay-rich silts and fine sands	Horizontally stratified layers	Overbank or tidal flat deposition at flood stage or high tide.
Fines with algae (Fa, was Fb)	Benthic algal mat and other limnic material	None visible to horizontal lamination	Lacustrine sediments
Organic, massive (Om)	Undecomposed organics, includes trace silt or sand layers	None visible	Autochthonous organic matter, fluvial sedimentation is rare or lacking. Omf, Omh, Oma can be used to subdivide fibric, hemic, and sapric classes
Organic, layered (Ol)	Undecomposed organic and fine mineral layers	Horizontal bedding, some alluvial mineral redistribution in peat	Occasional overbank deposition of suspended sediments
Organic, layered, turbated (Olt, unusual)	Undecomposed organic and mineral layers	Disrupted inclusions or inclined bedding due to cryoturbation	Interbedded sediments deformed by ice-wedge compression, layers still intact
Ice, vertical (Iv)	Pure ice, or nearly so, in ice wedges	Vertical striations in ice	Contraction cracking under cold temperatures
Ice, horizontal (Ih)	Pure ice, or nearly so, in horizontal layers	Horizontal striations in ice	Injection ice or water moving to freezing front

Appendix 2. Description of ground ice structures observed in the NPRA study area, 2003.

Class	Definition
Pore	Ice in minute holes, or pores, within mineral soil matrix that has an almost structureless appearance. May be visible (without handlens) or non-visible. Visual impression is that ice does not exceed original voids in soil. Forms where pore water freezes <i>in situ</i> .
Organic-matrix	Ice formed within organic matrix and has a structureless appearance. May be visible or non-visible. Mostly formed where pore water freezes <i>in situ</i> .
Crustal	Ice coating or rind around, or on the bottom of, a rock clasts or wood fragments.
Vein	Isolated, thin lens, needle-like or sheetlike structures, or particles visible in the face of soil mass. Usually inclined and bisecting sedimentary structures. Differs from layered ice in that they are solitary and do not have a repeated, parallel pattern.
Lenticular	Lens-shaped, thin (generally < 0.5 mm), short bodies of ice within a soil matrix. The orientation is generally normal to the freezing front and usually reflects the structure of the sediments.
Layered	Laterally continuous bands of ice less than 10 cm thick. Usually parallel, repeating sequences that follow with sedimentary structure or are normal to freezing front. Thicker layers (> 10 cm) are described as solid ice.  Sparse: ice layers <5% of structure. Medium: ice layers 5-25% of structure Dense: ice layers 25-50% of structure.
Reticulate	Net-like structure of ice veins surrounding fine-grained blocks of soil. Ice occupies up to 50% of surface area. Trapezoidal: ice has distinct horizontal parallel veins with occasional diagonal, vertically oriented veins. Soil blocks have trapezoidal appearance due to fewer vertical veins than lattice-like ice. An incomplete form of latticelike reticulate ice. Latticelike: ice exhibit regular, rectangular or square framework. Foliated: irregular horizontally dominated ice giving soil a platy structural appearance.
Ataxitic	Ice occupies 50-99% of cross-sectional area, giving the soil inclusions a suspended appearance. Sparse: ice occupies 50-75% area, soil inclusions occupy 25-50% of area. Medium Inclusions: ice occupies 75-95% of area, soil inclusions occupy 5-25%. Dense Inclusions: ice occupies 96-99% of area, soil inclusions occupy 1-5%.
Solid	Ice (>10 cm thick) where soil inclusions occupy <1% of the cross-sectional area. Clear Ice: no visible inclusions. Opaque Ice: cloudy or milky appearance. Dirty Ice: Individual soil grains, granules, or rock clasts visible but occupy <1% of area. Porous: ice contains numerous, interconnected voids, usually resulting from melting between air bubbles or along crystal interfaces from presence of salt or other materials in water. Though porous, the mass is firm or rigid. Columnar Ice: Ice that has melted or irradiated into long columnar crystals, very loosely bonded together. Stratified ice: Unspecified ice exhibits obvious banding or striations due to differences in color or sediment. Sheet ice: Cloudy or dirty, horizontally bedded ice exhibiting indistinct to distinct stratification. Wedge Ice: V-shaped masses of vertically foliated or stratified ice resulting from infilling of frost fissures. Best identified when large exposures or cross-sections are visible.